UNITED NATIONS UNIVERSITY
GEOTHERMAL TRAINING PROGRAMME
Orkustofnun, Grensásvegur 9,
IS-108 Reykjavík, Iceland

Reports 2008
Number 13

THE ISOTOPIC AND CHEMICAL CHARACTERISTICS OF GEOTHERMAL FLUIDS FROM THE WESTERN FJORDS, ICELAND AND TWO SELECTED HOT SPRING AREAS IN JIANGXI PROVINCE, SE-CHINA

Chen Gongxin
East China Institute of Technology
School of Civil and Environmental Engineering
Linchuan District, Fuzhou city, 344000
Jiangxi Province
P.R. CHINA
gxchen@ecit.edu.cn

ABSTRACT

Low-temperature geothermal activity is widespread in the Western Fjords, Iceland. The thermal waters are classified either as HCO_3 or Cl types. A few of the waters are mature according to a classification based on relative concentrations of HCO_3, SO_4 and Cl, and three of the waters samples fall within the zone of volcanic water. The Na-K-Mg triangular diagram suggests that some of the thermal waters have reached equilibrium and indicate reservoir temperature below 100°C. Boron and chloride concentrations and the B/Cl ratio suggest that the origin of these elements in the hot springs is, apart from the initial concentration of the precipitation, either leaching from rocks with which the water has reacted or due to seawater mixing. The $\delta^{18}O$ and δD ($\delta^{2}H$) are used to trace and determine the origin and movement of groundwater. All the waters follow a local meteoric water line ($\delta D = 6.55\ \delta^{18}O - 3.5$), indicating that the thermal waters are of meteoric origin. Some of the thermal waters are more depleted in δD than any current precipitation on the Peninsula. This may indicate that these waters have an older, ^{2}H depleted component from a colder climate regime. Radiogenic carbon ($^{14}C_{pMC}$) shows good correlation with water temperature, $\delta^{13}C$ and boron concentration. Earlier helium and carbon isotope study suggested that dilution of the mantle helium input occurs by addition of radiogenic helium and isotopically-light carbon from the uppermost crust.

Thermal waters from both Hengjing and Gangxi'nan geothermal areas are classified as HCO_3 type water. Na-K-Mg triangular diagrams indicate that the thermal waters from the Hengjing area are partially equilibrated or mixed waters, whereas those from the Gangxi'nan area are immature. The Na-K-Mg-Ca diagram indicates that temperature within the Hengjing geothermal reservoir is in the range of 130-180°C. The $\delta^{18}O$ and δD suggest that the thermal waters are of meteoric origin and that the recharge altitudes are at 350-800 m and 530-1460 m for the hot springs in Hengjing and Gangxi'nan, respectively. Helium and carbon isotopes from the Hengjing geothermal fluids (helium gas) show that they could be derived partly from the mantle, whereas those from the Gangxi'nan area is considered to be derived from the upmost crustal radiogenic production with addition of ^{13}C depleted carbon.

1. INTRODUCTION

It has long been recognized that chemical and isotopic compositions are important tools for studying the origin and history of geothermal waters. Hydrogen, oxygen and carbon isotopes play particularly important roles in determining the genesis of thermal waters and when studying the hydrodynamics of geothermal systems. These parameters are also important in identifying mixing processes between cold and thermal water, tracing groundwater movement and also in estimating the relative ages of thermal waters (Sveinbjörnsdóttir et al., 2000; Wang and Sun, 2001). Furthermore, in recent years, noble gas isotopes such as helium isotopes have been used to infer provenance of geothermal fluids (gas volatiles). Three areas, i.e. the Western fjords (NW-Peninsula), Iceland, and the Hengjing and Gangxi'nan geothermal areas in China, all of which are characterized by low-temperature activities, were selected for the present study. Although the three areas have very different geological and hydrogeological characteristics, the methods for geochemical studies are the same. In this report, the chemical compositions, hydrogen, oxygen and carbon isotopes and noble gas helium isotopes are used to study the origin and history of the thermal fluids.

In Iceland, oxygen and hydrogen isotopes have been widely used to trace groundwater movement and interpret the groundwater flow. They have been carried out in many areas during several past decades (Einarsson, 1942; Árnason, 1976, 1977; Sveinbjörnsdóttir et al., 1995, 1998, 2004). Deuterium content has been used to trace the origin of geothermal water in Iceland since the beginning of the 1970s (Árnason, 1976, 1977). At that time, it was generally assumed that GMWL was valid for Iceland. Based on more extensive oxygen and hydrogen isotope analyses and an isotopic ratio study, Sveinbjörnsdóttir et al. (1995) proposed a more suitable $\delta^{18}O$-δD relationship of the cold groundwater in Iceland with $\delta D = 6.5*\delta^{18}O-3.5$ for $\delta D \geq -10.5‰$ and $\delta D = 8*\delta^{18}O+11$ for lighter precipitation. Also, they suggested that the δD-values of present-day precipitation should be used with care to obtain information on the recharge areas to the various geothermal sites since the geothermal waters may contain a component of "ice age" groundwater, originating as precipitation in a significantly colder climate than that of today. In recent decades, both stable and radioactive carbon isotopes have been applied to study the Icelandic groundwater, including geothermal water (Sveinbjörnsdóttir et al., 1995, 2000, 2001, 2004, 2005; Sveinbjörnsdóttir and Arnórsson, 2007; Kristmannsdóttir and Sveinbjörnsdóttir, 1992). Sveinbjörnsdóttir et al. (1995) suggested a new correcting model for radiocarbon ages of groundwater based on the boron concentration of the waters. In the Western Fjords, geochemistry, particularly the chloride and boron concentrations, and stable isotopes of oxygen and hydrogen had previously been studied (Arnórsson, 1995). In 2003 and 2004 more detailed water sampling, including cold and warm waters, was carried out (Kristmannsdóttir et al., 2005). On the basis of this new dataset, together with the older data, a reinterpretation of the hydrogeological characteristics of the groundwaters, particularly thermal waters, is done in the present study. Hilton et al. (1998) suggested on the basis of helium and light carbon isotopes in gases escaping from thermal springs in the Western fjords, off-axis degassing of the hot spot.

In China, isotope studies also have a long history. These include oxygen and hydrogen isotopes of precipitation, and the application of isotope hydrological methodologies and isotope hydrological investigations of thermal waters, which have been studied since the 1970s (Wang and Sun, 2001). In Jianxi province, SW-China, isotope hydrogeological studies of groundwaters have been conducted in many geothermal areas (Li et al., 1992; Sun et al., 1992; Sun and Li, 2001). Local meteoric water lines, origins, recharge areas and the ages of the geothermal waters have been reported (Sun and Zhang, 2005). In recent years, the provenance of geothermal fluids has been suggested and new geothermal models have been established by applying gas compositions and carbon isotopes in some geothermal areas, as well as some noble gas isotopes, such as ^{3}He and ^{4}He (Sun and Li, 2001; Zhou and Zhang, 2001).

The main objectives of the present study are to compile all geochemical and isotopic data of both cold and warm waters from the Western fjords, Iceland, and the Hengjing and Gangxi'nan geothermal areas in China and interpret the water geochemistry with special emphasis on the following:

1. Chemical characteristics, including Cl and B, and classification of the thermal waters;
2. Interpretation of the stable isotopic composition and carbon isotopic composition of the natural waters to determine the origin, age and history of the thermal fluids;
3. Chemical and isotopic comparison of the three very different areas, regarding both geology and hydrogeology.

2. GEOLOGICAL BACKGROUNDS

2.1 The Western Fjords

The Western Fjords (the NW-Peninsula) are located in NW-Iceland and comprise the biggest peninsula in Iceland. The geographical position of the area is indicated on Figure 1 where a simplified geological map of Iceland is shown. The area is a 500-600 m high basalt plateau intersected by several deep, glacially eroded valleys and fjords. The geology of the Western Fjords is characterized by Miocene flood basalts. Geological studies indicate that most of the basalt pile is composed of tholeiitic lavas of varying thicknesses, interbedded with soil layers. The lava pile has a regional dip of 3-7° towards the southeast and ranges in age from about 16 M.y. at the western margin to about 9 M.y. in the southeast (McDougall et al., 1984; Hardarson et al., 1997). The lava pile is cut by dykes and faults with a dominant NE-SW orientation, parallel to the strike direction. Benjamínson (1981) showed that hydrothermal manifestations are widespread in the area and that the location of the hot springs is controlled by dykes and faults. The surface hydrothermal activity in this part of Iceland is classified as low-temperature activity, from just above ambient temperature up to 100°C. Flow rates are also variable but natural flows extend up to ~5 l/s. The regional thermal gradient varies from 50°C km^{-1} in the west to about 70°C km^{-1} in the east. There is though a temperature anomaly (gradient over 100°Ckm^{-1}) to the south of the peninsula (Pálmason and Saemundsson, 1979). Water penetration and circulation to depths of 1-3 km can account for the thermal activity (Fridleifsson, 1979; Arnórsson, 1995).

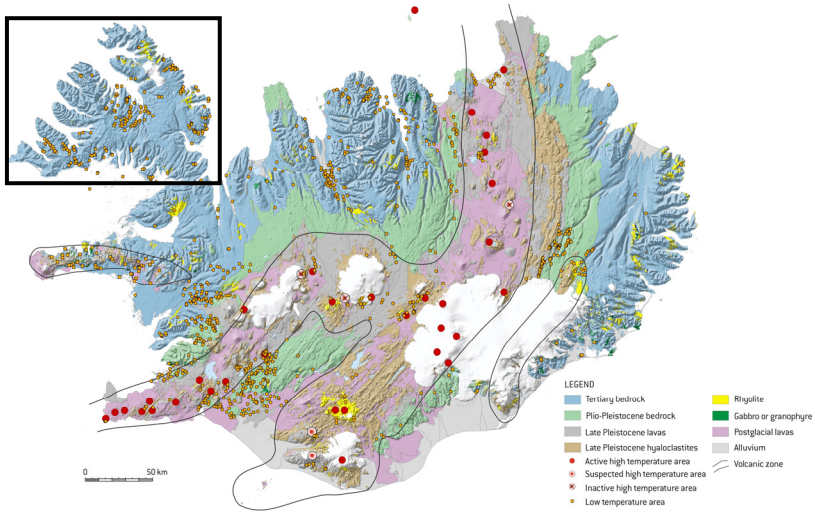

FIGURE 1: A simplified geological map of Iceland (Jóhannesson and Saemundsson, 1999); the box covers the Western Fjords, the target area in Iceland in this study. Red circles denote high-temperature activity and yellow circles low-temperature activity

2.2 Geothermal areas in Jiangxi province, SE-China

Jiangxi Province, SE-China, is one of the provinces in which hot springs are most widely distributed in China (Sun, 1998). Two important geothermal areas in the province, namely Hengjing and Gangxi'nan, were selected for this study. Two types of hot springs, some with a remarkable amount of gas escaping, and others with unusually high temperatures are found within these two areas. Two

investigations performed in 1997 and 2003 were done to study the occurrences of geothermal fluids and to assess the geothermal reservoirs (Sun and Zhang, 2005).

2.2.1 The Hengjing geothermal area

The Hengjing geothermal area is located in Xunwu County, South Jiangxi Province and has more hot springs than any other area in the province. Many of the hot springs are characterized by CO_2 and other escaping gases. Their temperatures are in the range of 26-73°C at the surface. A simplified geological map of the Hengjing area is shown in Figure 2. The rock matrix consists mainly of the upper Cretaceous system (K_2) characterized by red sandstone and conglomerate, the lower Jurassic system (J_1) and the upper Jurassic system (J_3) by sandstone and conglomerates, the Sinian-Cambrian system (Z-∈) by metamorphic sandstone, and migmatite as well as the Yanshannian granite (γ_5^2) and biotite-granite ($\pi\gamma_5^2$) (Figure 2). Since the 1960s, geological and hydrogeological surveys have identified 13 thermal springs in the area, located along northeasterly trending faults, but also controlled by northwesterly faults (Sun and Zhang, 2005). These faults are well developed in the area. From 1974 to 1992, more than 30 earthquakes occurred. One of the biggest occurred in August, 1987, with a magnitude of 5.7. The earthquake activity is indicative of that these faults are still active. The average terrestrial heat flow of 74.1 mW/m^2 is somewhat higher than the average value of 69.8 mW/m^2 for the whole province (Li and Zhou, 1992).

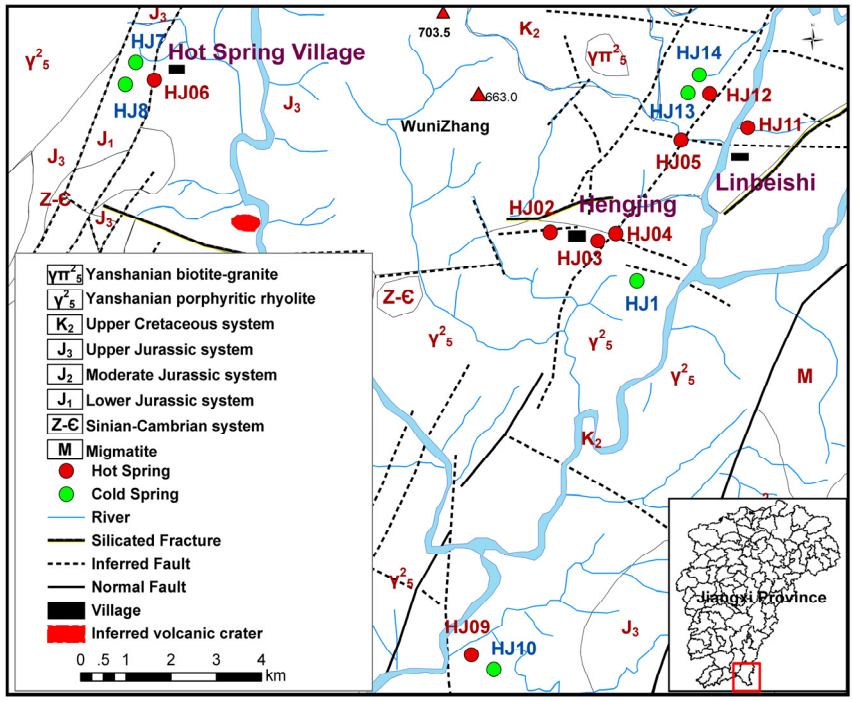

FIGURE 2: The geological map of Hengjing geothermal area (Sun and Zhang, 2005)

2.2.2 The Gangxi'nan geothermal area

The Gangxi'nan geothermal area is located in SW-Jiangxi Province, covering almost five counties including Dayu, Chongyu, Shuicuan and Shanyu as shown in Figure 3. The rock types developed in this region are mostly the same as in the Hengjing Area, consisting largely of the Cretaceous system (K) characterized by sandstone and conglomerate, the Jurassic system (J) - sandstone, conglomerates and tuff, and migmatite as well as the Yanshannian granite. Hydrothermal manifestations are widespread in the area and faults exert localized control over the surface distribution of hot springs. The faults involve two major fault trends, north-northeasterly and east-northeasterly. More than 10 hot springs have been found with temperatures ranging from 37.7 to 83.8°C at the faults' southern ends. Five of the springs have escaping gases.

3. METHODOLOGY

3.1 Natural isotopes

Isotopes have become an essential part of studies of major geothermal development. Their use and interpretation are strengthened if complemented and combined with chemical techniques.

3.1.1 Oxygen and hydrogen isotopes

Oxygen and hydrogen isotopes are widely used in geothermal studies. They are extensively applied to determine the origin and history of geothermal fluids and most often serve as natural tracers for the provenance of geothermal water. Isotopic studies have shown that geothermal water is most often of meteoric origin (Craig, 1961, 1963). Craig (1961) observed that the $\delta^{18}O$ and δD values in precipitation are linearly related by:

$$\delta D = \delta^{18}O + 10 \quad (1)$$

where the values δD and $\delta^{18}O$ are obtained with the following equation:

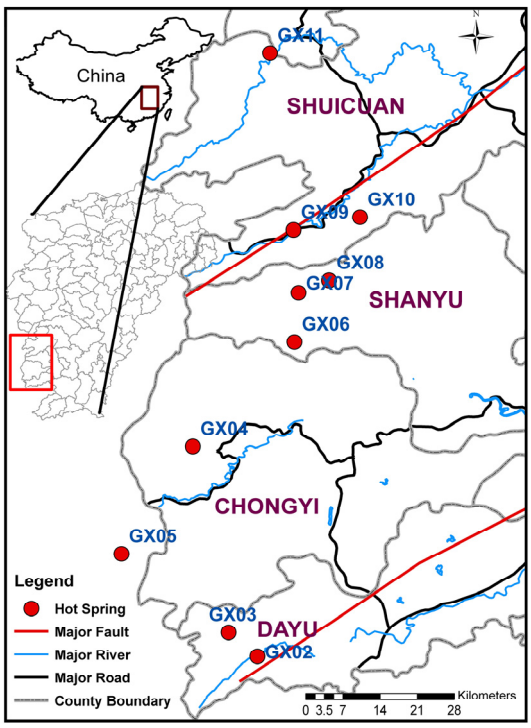

FIGURE 3: Geological map of the Gangxi'nan geothermal area showing major faults and thermal water sampling locations

$$\delta = \frac{R_{sample} - R_{standard}}{R_{standard}} \times 1000 \quad (2)$$

where R stands for the isotopic ratio (e.g. $D/^{1}H$ or $^{18}O/^{16}O$) of the sample or the standard.

The standard that has been used for measuring delta values for the oxygen and hydrogen isotopes in water is the Standard Mean Ocean Water (SMOW). By definition, SMOW has the values $\delta^{18}O = 0‰$ and $\delta D = 0‰$. The line defined by Equation 1 is termed the "World meteoric water line" (WMWL) or "Global meteoric water line" (GMWL), and is based on precipitation data from locations around the globe. The isotopic characteristics ($\delta^{18}O$ and δD) of precipitation are related to latitude and continental effects. Thus $\delta^{18}O$ and δD decrease from the tropics to the poles and from coastal to inland areas. There are also seasonal fluctuations as well as an altitude effect – a decrease of ^{18}O and D concentrations with increasing elevation. The relationship provides a useful reference for geothermal studies in helping to identify recharge areas to geothermal systems. Local meteoric waters in different geographical areas can, however, have different meteoric water lines. The slope and intercept of any "Local meteoric water line" can be significantly different from the "Global meteoric water line".

Some subsurface processes can change the original isotopic characteristics of geothermal waters. Isotopic exchange at high temperature between the water and the rock minerals can lead to an increase in the ^{18}O content of the water and a decrease in the ^{18}O content of the rock. This causes the "oxygen isotope shift" in the $\delta^{18}O$-δD diagram, towards less negative values of $\delta^{18}O$ (Ellis and Mahon, 1977). Reactions of rocks with seawater or reservoir water at low to intermediate temperatures can cause a less common shift of $\delta^{18}O$ away from the meteoric water line towards more negative values (Nicholson, 1993). Generally, no corresponding shift is seen in the δD value, because there is little hydrogen in the rocks relative to that in the water. However, in systems where there is a large proportion of clay and micaceous minerals, some exchange of deuterium with hydrous minerals can occur, making possible a slight "deuterium shift" (Ellis and Mahon, 1977). Mixing with local

meteoric water can change the isotopic composition of geothermal fluids. The $\delta^{18}O$ and δD ratios can provide an indication of boiling as well as mixing processes in the geothermal system.

3.1.2 The carbon isotopes ^{14}C and $\delta^{13}C$

There are three major carbon isotopes existing in nature, ^{14}C, ^{13}C and ^{12}C. The ^{14}C isotope is radioactive while ^{12}C and ^{13}C are stable. The ^{14}C isotope with its half-life of about 5700 years, offers the potential of dating groundwater (Mook, 1980, Sveinbjörnsdóttir et al., 1998). The $\delta^{13}C$ is defined as δD and $\delta^{18}O$ by Equation 2 and is useful for indicating the sources of fluids (gas and liquid). Different ^{14}C and ^{13}C concentrations may indicate that carbon in groundwater is derived from several sources. Age determination of groundwater is complex from a geochemical point of view, and the interpretation of ^{14}C determination is often unclear. Whereas, under certain conditions, absolute groundwater ages can be obtained within certain limits by applying correction procedures using the chemical and stable carbon isotopic composition of the sample (e.g., Dörr et al., 1987; Aravena and Suzuki, 1990; Aravena and Wassenaar, 1993; Taylor, 1994; Sveinbjörnsdóttir et al., 1998). Also because of the presence of large quantities of ^{14}C free volcanic CO_2 in most geothermal systems and an exchange with $CaCO_3$, ^{14}C is a complex parameter to use in geothermal projects (Arnórsson, 2000). Relative ^{14}C ages can, however, be determined with more certainty. Both in Iceland and China, at least three different sources of carbon supply are in the thermal water, atmospheric CO_2, soil CO_2 of organic origin and CO_2 leached from the rock through which the water seeps. Moreover, there may be a supply of CO_2 from a magmatic source in some geothermal systems (Sveinbjörnsdóttir et al., 1998; Dai and Dai., 1994). Earlier studies have shown that the $\delta^{13}C$ values in cold surface waters in Iceland range from -1 to -7‰, whereas in soil waters the $\delta^{13}C$ is much lighter and ranges from -16 to -22‰. In geothermal waters, the values usually fall in the range -6 to -13‰ (Sveinbjörnsdóttir et al., 2000). The average $\delta^{13}C$ value for atmospheric CO_2 is close to -7‰, the organic decay CO_2 is close to -25‰ and CO_2 leached from the rock is close to -1‰ for limestone of marine origin and -5‰ for MORB (mid-ocean ridge basalt) (Hilton et al., 1998). Accordingly, mixing of carbon of different origins with the thermal fluids can change the carbon content of the fluids drastically.

3.1.3 Noble gas isotopes ^{3}He and ^{4}He

Noble gas isotopes are often used in geochemistry. Helium is one of the most important noble rare gases in geothermal fluid. There are two major isotopes of He, ^{3}He (abundance 1.37×10^{-4} %) and ^{4}He (abundance >99.99 %). In recent decades, helium isotopes have been used successfully as tracers for mantle volatile degassing and, hence, to study the source of geothermal fluids. The ^{3}He isotope in geothermal fluids can be derived from several different sources, such as mantle, crust, subducted sediments or the atmosphere. Thus, these isotopes are very useful in indicating the source of associated thermal fluids (Arnórsson, 2000). ^{3}He is generally considered to have a primitive origin, produced from nuclear fusion reaction and captured by cosmic nebula. Presently, ^{3}He exits mostly in the mantle, that is to say, mantle source is probably the major ^{3}He source on earth. The ^{4}He isotope is a radiogenic isotope and is produced through decay by uranium and thorium in the crust. According to this, the $^{3}He/^{4}He$ ratio can be used to indicate the genesis of fluids, where low helium ratios indicate fluids of crustal source and the higher values indicate a mantle source. The represented helium ratio value (Ra) of a meteoric source is 1.4×10^{-6}, the crust has 2.0×10^{-8} and the mantle 1.1×10^{-5} (Wang, 1989). Conveniently, the ratio (R/Ra) of $^{3}He/^{4}He$ between a sample (R) and the air (Ra) is used to reflect the fluid source. Normally, if $R/Ra < 1$, He is considered to be of crustal radio-genesis, whereas, if $R/Ra > 1$, it has been accompanied by the addition of mantle degassing. According to Hilton et al. (1998), three typical R/Ra values are reported worldwide. The highest value is 30 and matches the most extreme magmatic ratio. The second is 8±1 – MORB (the mid-ocean ridge basalt) helium ratio, and the third is 0.05 (or 0.01-0.1) indicating a significant proportion of radiogenic production, i.e. crustal origin. These typical values are used to identify sources of geothermal fluids in the present study.

3.2 Chemical features of the fluid

3.2.1 Cl-SO_4-HCO_3 triangular diagram

The Cl-SO_4-HCO_3 ternary diagram is one of the diagrams used for the classification of natural waters (Giggenbach, 1988). It helps to discern immature unstable waters and gives an initial indication of mixing relationships or geographical groupings. The diagram distinguishes several types of thermal water including immature waters, peripheral waters, volcanic waters and steam-heated waters. It gives a preliminary statistical evaluation of groupings and trends. The position of a data point in such a triangular plot is simply obtained by first forming the sum *S* of all three constituents involved (in mg/kg), or:

$$S = C_{Cl} + C_{SO4} + C_{HCO3} \tag{3}$$

Then the percentage of each of the three anions can be calculated as:

$$Cl\ (\%) = \frac{C_{Cl}}{S} \times 100\ ;\ SO_4\ (\%) = \frac{C_{SO4}}{S} \times 100\ ;\ HCO_3\ (\%) = \frac{C_{HCO_3}}{S} \times 100 \tag{4}$$

3.2.2 Na-K-Mg triangular diagram

The Na-K-Mg diagram is used to classify waters into fully equilibrated, partially equilibrated and immature waters. It can be used to predict the equilibrium temperature and also the suitability of thermal waters for the application of ionic solute geothermometers. It is based on the temperature dependence of the full equilibrium assemblage of potassium and sodium minerals that are expected to form after isochemical recrystallization of average crustal rock under conditions of geothermal interest (Giggenbach, 1988, 1991). Essentially, it is based on the temperature dependence of the two reactions:

$$K\text{-}feldspar + Na^+ = Na\text{-}feldspar + K^+ \tag{5}$$

$$0.8\ K\text{-}mica + 0.2\ chlorite + 5.4\ silica + 2\ K^+ = 2.8\ K\text{-}feldspar + 1.6\ H_2O + Mg^{+2} \tag{6}$$

Na, K and Mg concentrations of waters in equilibrium with this assemblage are accessible to rigorous evaluation. The coordinates of a point on the diagram are calculated by

$$S = C_{Na}/1000 + C_K/100 + C_{\sqrt{Mg}} \tag{7}$$

$$\%Na = C_{Na}/10S \quad \%K = C_K/S \quad \%Mg = C_{\sqrt{Mg}}/S \tag{8}$$

4. SAMPLING AND ANALYTICAL METHODS

Sample collection, chemical analysis and data interpretation are the three main steps involved in geochemical studies of geothermal fluids. A brief description of the sampling techniques, sample treatment and analytical techniques adopted here is given in this section. For detailed water chemical sampling and analytical techniques, see Paces (1991), Arnórsson (1991), D'Amore and Arnórsson (2000), Ármannsson and Ólafsson (2000) and Pang and Ármannsson (2006), and for detailed isotopic chemical sampling and analytical techniques, see Sveinbjörnsdóttir et al. (1995, 1998, 2000), Hilton (1996) and Hilton et al. (1998).

4.1 Sampling

In this study, water samples and gas samples from cold and hot springs and from hot water wells are used. The collection of representative gas samples for isotopic analysis from a discharging spring involves the collection of dry gas (volatile). In this report, several data sets were used which were made available for the present study. Some of the data have previously been published:

The Western Fjords: The "newer dataset" includes both cold and thermal waters samples that were collected in 2003 and 2004 and were provided by Kristmannsdóttir et al. (2005). This dataset is unpublished. Others data are older, and referred to as "older datasets", both from cold and thermal waters and sampled in the years from 1979 to 1990 (Arnórsson, 1995). The helium isotopic data were obtained from a published paper by Hilton et al. (1998). The data are seen in Table 1 in Appendix I.

The Hengjing and Gangxi'nan geothermal areas: These waters were sampled in 1997 and 2003, respectively, under a project which was funded by a grant from the National Natural Science Foundation of China (40472147). Some of the data have been published (Sun and Li, 2001; Sun and Zhang 2005; Zhou and Zhang, 2001). The data are presented in Tables 2 and 3 in Appendix I.

4.2 Analytical methods

The analytical methods, including water chemistry and isotopes, used to obtain data for the report are presented in Table 1.

TABLE 1: Analytical methods for chemical analyses and isotopes of natural waters

Composition	Sample fraction	Methods of analysis
CO_2	Ru	Alkalinity-titration
H_2S	Ru	Titration
SiO_2	Rd	Spectrophotometry
Na	Fa	Atomic absorption spectrometry
K	Fa	Atomic absorption spectrometry
Ca	Fa	Atomic absorption spectrometry
F	Ru	Ion selective electrode
Cl	Ru	Ion chromatography
SO_4	Fp	Ion chromatography
Al	Fa	Atomic absorption spectrometry
Fe	Fa	Atomic absorption spectrometry
B	Fa	Modification of the curcumin
pH	Ru	Ion selective electrode
$\delta^{18}O$, δD, $\delta^{13}C$	Ru	Mass spectrometry (Finnegan MAT-251, MAT-252)
^{14}C	Gas	AMS (Accelerator Mass Spectrometer)
^{3}He,^{4}He	Gas	Va 5400, MAP 215 rare gas mass spectrometer

The oxygen and hydrogen isotopic composition of groundwater was analyzed and the data are represented as δ-values in per-mil. Oxygen was extracted from the water by equilibrating 5 ml of degassed water with small amount of CO_2 gas in a sealed tube for 3 hours in a shaking water bath at 20.0°C (Epstein and Mayeda, 1953). The measurements were subsequently corrected for the CO_2 gas which is also used as the secondary reference standard. In Iceland, hydrogen isotope analysis based on the zinc reduction method (Coleman et al., 1982) was used until 1998 but later by the H_2-water equilibration method using a Pt-catalyst (Horita, 1988). The samples from the Western Fjords, Iceland were analyzed, on the Finnegan MAT 251 at the Science Institute, University of Iceland. The accuracy of the measurements, at the 95% confidence level, is 0.04‰ for $\delta^{18}O$ and 1.0‰ for δD. The samples from the Hengjing and Gangxi'nan areas in China were analyzed on the Finnegan MAT252 at

the National Lad., Nanjing University. The accuracy of the measurements is better than 0.2‰ for $\delta^{18}O$ and 3‰ for δD.

The sample preparation for carbon isotopes was carried out in accordance to McNichol et al. (1994), i.e. the water samples (1 litre) were acidified in a vacuum system and CO_2 was extracted directly by nitrogen flow through the water sample. The collected CO_2 was then partly used for $\delta^{13}C$ measurements performed at Finnegan MAT 251 mass spectrometer at the Science Institute, University of Iceland and partly converted to graphite for AMS ^{14}C measurements at the Aarhus EN tandem accelerator, Denmark (Sveinbjörnsdóttir et al., 1992). The ^{14}C results were normalized to a $\delta^{13}C$ value of -25‰ PDB and expressed in "percent modern carbon" (pMC) relative to 0.95 times the ^{14}C concentration of NBS oxalic acid (HOxI) (Sveinbjörnsdóttir et al., 1995, 2000). The released CO_2 from the Hengjing and Gangxi'nan areas was measured only for $\delta^{13}C$ at the Finnegan MAT 252 mass spectrometer at the Lanzhou Institute of Geology, Chinese Academy of Sciences. The accuracy of the measurement is better than 0.1‰ (PDB).

Helium isotope data are available for the Hengjing and Gangxi'nan areas in China (Zhou and Zhang, 2001) and also for the Western Fjords, Iceland (Hilton et al., 1998). In China, sample collection took place over two periods (1997 and 2003) following closely the standard sampling techniques as described by Hilton (1996). All samples were collected in AR-glass flasks with prolonged flushing of all connecting tubing, carried out to ensure minimal atmospheric contamination. The helium isotope ratio of the volatile for the Chinese samples was analyzed on the VG5400 at the Lanzhou Institute of Geology, Chinese Academy of Sciences, China. The accuracy of $^4He/^3He$ measurement is better than 0.3×10^{-6}%. The samples from the Western Fjords, Iceland were analyzed on MAP 215 rare gas mass spectrometer in Berlin using gas preparation.

5. CHEMICAL AND ISOTOPIC CHARACTERISTICS OF THE THERMAL FLUIDS

5.1 The Western Fjords in Iceland

5.1.1 Chemical characteristics of the waters

From the Western Fjords, 101 samples have been collected over seven time periods. In 2003 and 2004, 37 samples were collected, characterized as "newer dataset". The other 64 samples were collected in 1979, 1985, 1987, 1989 and 1990, respectively, characterized as the "older dataset" in this study. All the samples were taken from steam, thermal springs, and from shallow cold water and thermal wells. Geologically and geographically, the sample localities were subdivided into four sub areas (subarea 1, 2, 3 and 4) (the distribution can be seen in Figure 10). Partial analyses of the samples are given in Table 1 in Appendix I, together with the oxygen, hydrogen and carbon isotopic composition. The temperatures of the waters range from 2 to 100°C.

All the geothermal waters in the Western Fjords are relatively dilute. The TDS content of the waters most often lies in the range of 10-150 ppm. A classification of the waters was carried out on the basis of relative contents of the three major anions, Cl, SO_4 and HCO_3, as shown in Figure 4a. Three of the water samples plot in the field marked "volcanic water" in this diagram, and only a few water samples plot in the "mature water" area. More than half of the water samples contain chlorine ion as the dominant anion, while less the than half contain HCO_3 as the predominated anion. This may indicate that in some places the thermal water is mixed with seawater. Sodium and potassium are the dominant cations in both cold and geothermal waters as shown in Figure 4b and silica is always an important constituent.

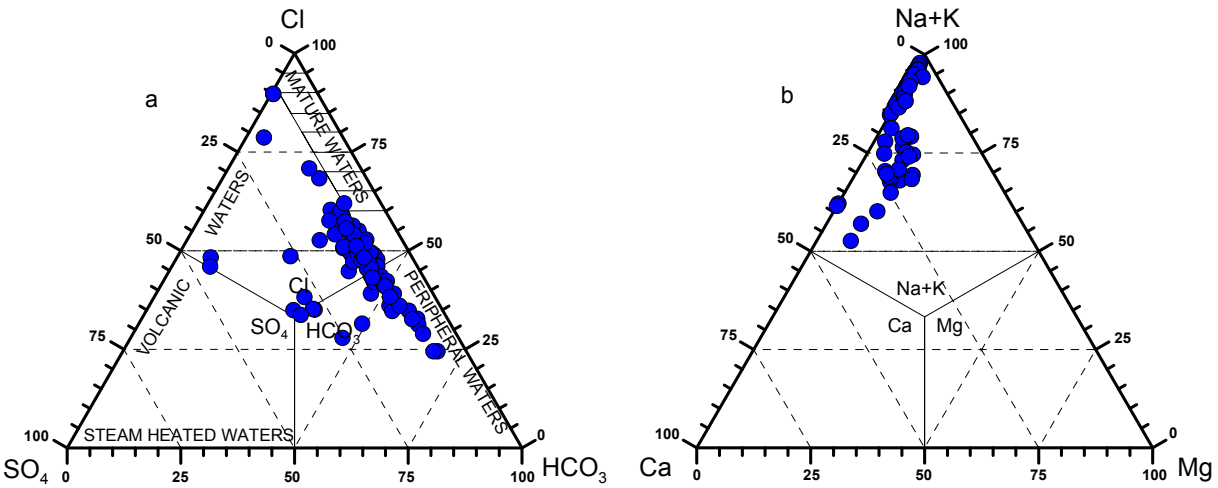

FIGURE 4: Classification of waters from the Western Fjords on the basis of a) Relative Cl, SO_4 and HCO_3 content (in ppm); b) Relative Ca, Mg and Na+K content (in ppm)

Some of the data of thermal water from the Western Fjords have been plotted on the Na-K-Mg ternary diagram (Figure 5). Most of the hot spring waters plot in the √Mg corner, which means that these waters have not attained equilibrium and are immature. This may indicate that the water is young and has not reacted for a long time with the bedrock or may have mixed with cold water in the upflow zone. However some of the waters have reached full equilibrium. For the mature waters, the estimated discharge temperature is in the range of 75-100°C, indicating that the temperature of the geothermal water at depth is not high and thus the area is classified as a low-temperature area.

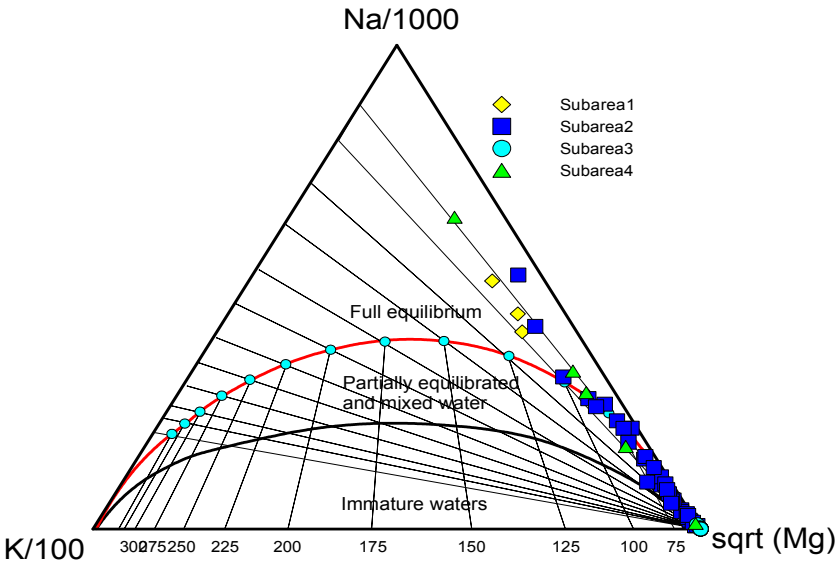

FIGURE 5: Na-K-Mg equilibrium diagram (Arnórsson, 2000) for the fluids from the Western Fjords; the waters from subarea 1 are represented by diamonds, subarea 2 by squares, subarea 3 by circles, and subarea 4 by triangles

The concentration of Cl in cold water (<10°C) lies in the range of 3.7-32 ppm and that of B in the range of 0.0018-0.0152 ppm (Figure 6). The Cl/B ratios are similar to those of seawater or slightly lower, ranging from 413 to 1626. The slope (Cl/B ratio) of the line through the cold water data points is about 1302, i.e. very close to the ratio of seawater (Figure 6). The Cl concentrations and the Cl/B ratios of the cold waters suggest the source of supply of Cl and B is for the most part the ocean, seawater spray and aerosols brought down with the precipitation (Arnórsson and Andrésdóttir, 1995). In the thermal water the B and Cl concentrations are somewhat higher due to water rock interaction (Figures 6 and 7). All the thermal samples seem to follow broadly the same line except for subarea 1 where the samples are relatively high in Cl compared to B (Figure 6).

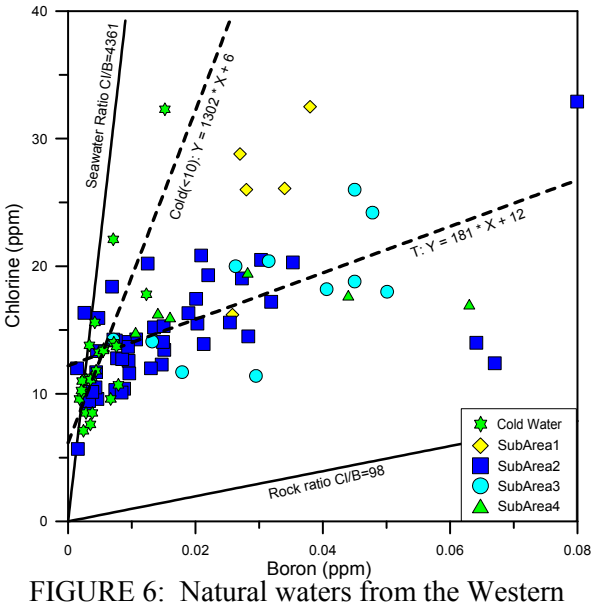

FIGURE 6: Natural waters from the Western Fjords and relationship between the Cl and B concentrations; the dash line T is given by Y = 181*X + 12, represents the best fit for all the thermal data; while the dash line cold (T<10°C) given by Y = 1302*X + 6 represents the best fit line for the cold water from the area

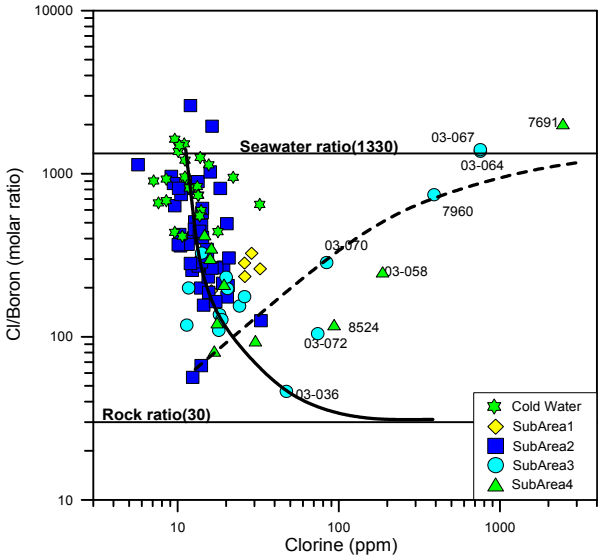

FIGURE 7: Cl-B relationship for natural waters from the Western Fjords; the solid curve represents Cl/B-Cl relationship in water with initial 15 ppm Cl and Cl/B molal ratio of 1330, which subsequently gained Cl and B by rock dissolution in the ratio of 30; and the dash curve corresponds to a mixture of seawater and water containing 15 ppm Cl with a Cl/B molal ratio of 30

The slope (Cl/B ratio) of the line through the thermal data points is 181, which is much lower than that for seawater Cl/B ratio (Figure 6). This ratio is also significantly higher than Cl/B ratios in most analysed basalts in Iceland (~30) (Arnórsson and Andrésdóttir, 1995). The intercept with the line representing the Cl/B ratio in cold water is 12 ppm indicating that this is the average Cl content of the precipitation from which the thermal waters are derived.

The effect of rock dissolution on changes in aqueous Cl/B ratio is depicted by the solid line curve in Figure 7 for initial Cl concentrations of 15 ppm in the parent meteoric water. In calculating these curves, it was assumed that the Cl/B molal ratio of the rock was 30 and that these elements were dissolved in stoichiometric proportions. Mixing of marine groundwater with the geothermal water will cause increases in both in Cl/B ratios and Cl concentrations but have little effect on B concentrations unless the marine groundwater component in the geothermal water is relatively large. The broken line in Figure 7 shows how Cl concentrations and Cl/B ratios change as water with an initial Cl/B molal ratio of 50 and Cl concentration of 15 ppm mixes with seawater. Most of the data points in Figure 7 fall close to the rock dissolution line, whereas some, mainly from subarea 3 and 4, show subsequent mixing with seawater. This is in agreement with Arnórsson and Andrésdóttir (1995) which suggested that these two processes, i.e. rock dissolution and seawater mixing, control the distribution of Cl and B in geothermal waters.

5.1.2 Stable isotopes of oxygen and hydrogen

The stable isotopic compositions of oxygen and hydrogen in water samples from the Western Fjords are shown in Appendix I. The δD and $\delta^{18}O$ values are in the range of -84 to -56‰ and -12 to -8.2‰, respectively. All the data are plotted in Figure 8 and shown with two types of symbols, circles representing the "older dataset", sampled 15-20 years ago, and the squares representing water samples collected in 2003 and 2004. Some of the samples in the "newer dataset" are collected at the same localities as the older ones. For those samples, no significant isotopic changes have occurred during the last 20 years. Most of the newer samples are, though, collected in different places and these

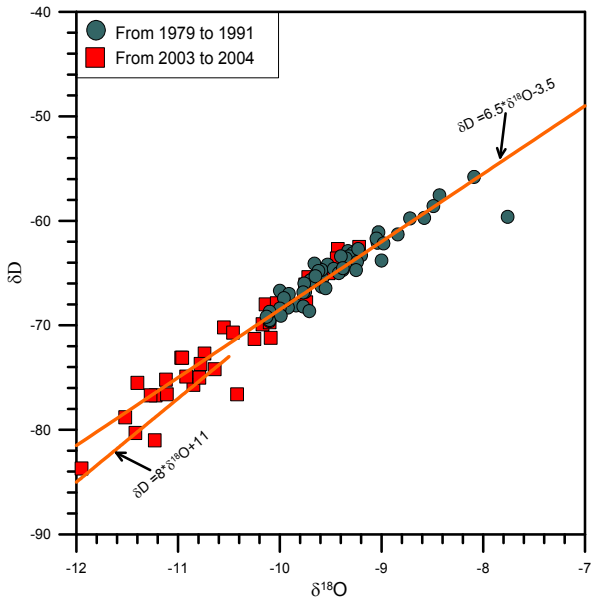

FIGURE 8: The relationship between δD and $\delta^{18}O$ for waters from the Western Fjords; the "older dataset" is represented by circles, and the "newer dataset" by squares

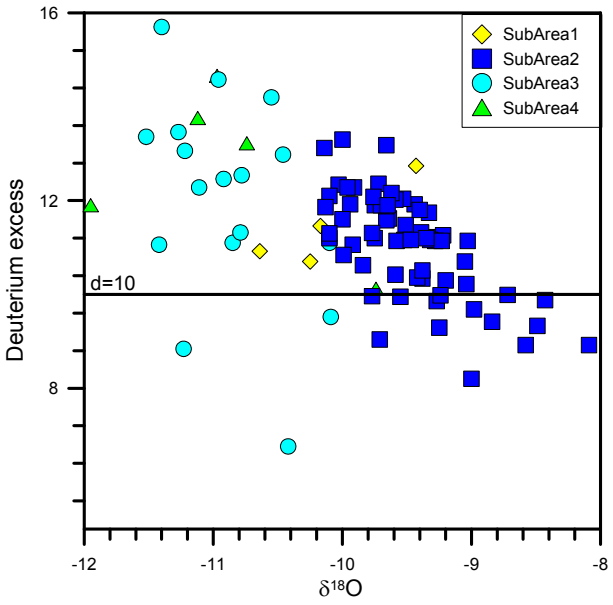

FIGURE 9: The natural waters of the Western Fjords and their relationship between deuterium excess (d = δD - 8*$\delta^{18}O$) and $\delta^{18}O$

samples are generally more depleted in ^{18}O and D than the older samples. Water samples collected in different areas have different isotopic content because their sub groundwater systems are relatively independent.

In 1995, Sveinbjörnsdóttir et al. defined the local meteoric water lines for Iceland, by:

1) $\delta D = 6.55\ \delta^{18}O - 3.5$
when $\delta^{18}O > -10.5‰$;

2) $\delta D = 8\ \delta^{18}O + 11$
when $\delta^{18}O < -10.5‰$.

As shown in Figure 8, the light isotopic data from the Western Fjords seem to fit better with line 1 than line 2. No oxygen shift is observed indicating that the temperature of the deep geothermal waters is not high.

The deuterium excess (d) is defined as $\delta D - 8*\delta^{18}O$. When oxygen shift is not observed, the deuterium excess of the groundwater is a good indicator for further information of the origin of the water (Sveinbjörnsdóttir and Arnórsson, 2007). As seen in Figure 9 the deuterium excess is quite variable and lies mostly in the range from 8 to 16‰. These values are somewhat higher than for water in a tropical high-humidity area, which has d value of 8‰ (5), but on the other hand, much lower than for water in the dry east Mediterranean region, with d value of +22‰. Figure 9 shows a clear linear relationship between $\delta^{18}O$ and d-values, where the most ^{18}O-depleted samples (i.e. most negative $\delta^{18}O$) have the highest d-values. Johnsen et al. (1989) showed that the d-values depend on the relative humidity at the source area of the precipitation. The higher d-values of samples with the most negative $\delta^{18}O$ values suggest that the water originates from a region with low humidity.

Deuterium of the mean annual precipitation in Iceland was mapped in the 1970s, allowing deuterium to be used to delineate regional movement of groundwater (Árnason, 1976, 1977; Tómasson et al., 1975; Sveinbjörnsdóttir et al. 1995). In the present study, 91 samples of both cold and warm waters collected all through the Western Fjords were made available. In the deuterium map (Figure 10), the isotopic composition of the mean annual precipitation for the Western Fjords is shown (Árnason, 1976) as contour lines and compared with the isotopic composition of individual samples. Most of the samples in the older dataset were collected in subarea 2, while most of those in the newer dataset are located within the other three sub areas. Samples of thermal waters in subarea 1 in the southern part of the Western Fjords give deuterium values in the range of -63 to -74‰. According to the deuterium map, the isotopic values of thermal

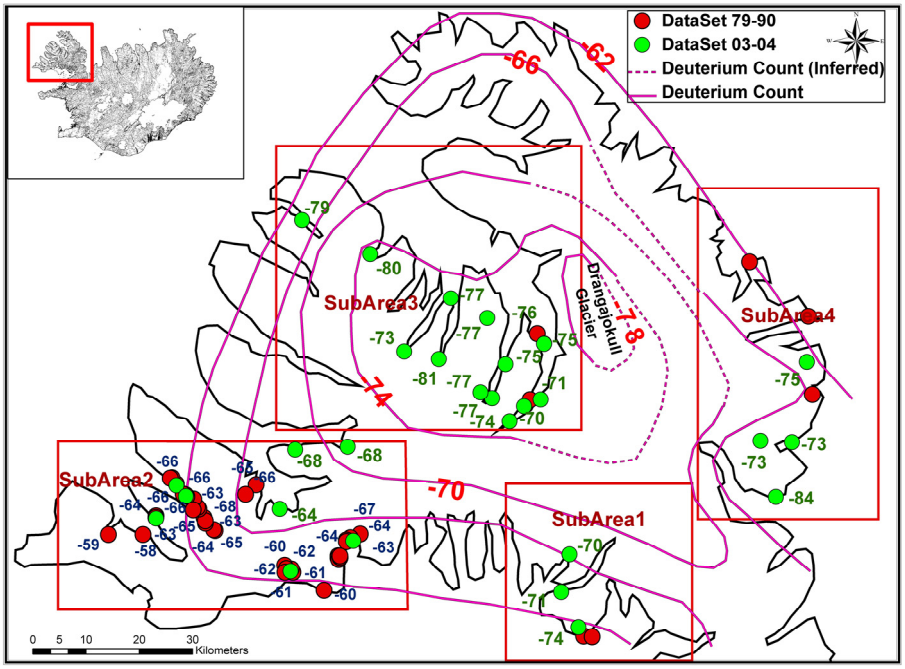

FIGURE 10: The deuterium isotope variations for the Western Fjords thermal fluid; δD contours (from Árnason, 1976) for localized precipitation are shown for comparison

waters are similar to deuterium values of local precipitation found in the highland about 30 km north to subarea 1. In the eastern coastal subarea 4, the deuterium content of the thermal water ranges from -73 to -84‰. The most negative values are lower than any local precipitation on the NW-Peninsula today, according to Árnason (1976). The deuterium content of hot springs in the western coastal subarea 2 is in the range of -58 to -65‰ and is less negative than waters in the other sub areas. This observation is consistent with a localized origin for the thermal waters. The deuterium values of hot springs in subarea 3 are in the range of -70 to -81‰. It is suggested that the warm waters originate as precipitation in the mountainous areas close to the springs, except for the most negative values (such as samples 03-066, 03-072, 03-070) that are likely to have a more distant recharge area.

The most depleted samples (samples 03-066, 03-072 and 03-070), including one sample 03-058 from subarea 4, have more depleted values in deuterium than the most depleted value (δD = -78‰) of the mean annual precipitation in the Western Fjords given by Árnason (1976). This suggests that either the contour map by Árnason is not accurate enough because of insufficient data in the 1970s or they may have a component of old ice age water that is more depleted due to the cold climate at that time. Most of these samples are also exceptional in their chemistry, both in chlorine and boron. This can be seen more clearly in Figure 11. The relationship between δD and chlorine is seen in Figure 11a, and shows increasing Cl concentration with decreasing δD, except for sample 03-066 which is very low in Cl concentration; The relationship between δD and boron is seen in Figure 11b. As demonstrated in Figure 7, the Cl rich thermal waters gained their Cl concentration by mixing with seawater. These sample sites are close to the shore and seem to be characterized by fractures extending into the ocean. Thus, when the thermal waters ascend, they mix with seawater, which flows directly from the ocean through these fractures. This can account for the presence of the seawater component in the thermal water.

5.1.3 Carbon isotopes of the thermal water

Figure 12a shows the relationship between temperature and ^{14}C age (as Percentage of Modern Carbon, PMC). The data can be subdivided into two groups, the cold water group, which is encompassed by circles, with temperature less than 10°C and the thermal water group. The figure suggests a negative relationship between temperature and modern ^{14}C concentration, where the modern ^{14}C concentration decreases with increasing water temperature. This suggests that the higher temperature waters are of older ages and they reflect more intense water-rock interaction. A similar trend is observed for the relationship between the ^{13}C concentration and modern ^{14}C concentration of the thermal water, if the cold water and sample 04-019 point are kept apart (Figure 12b). A possible explanation for the

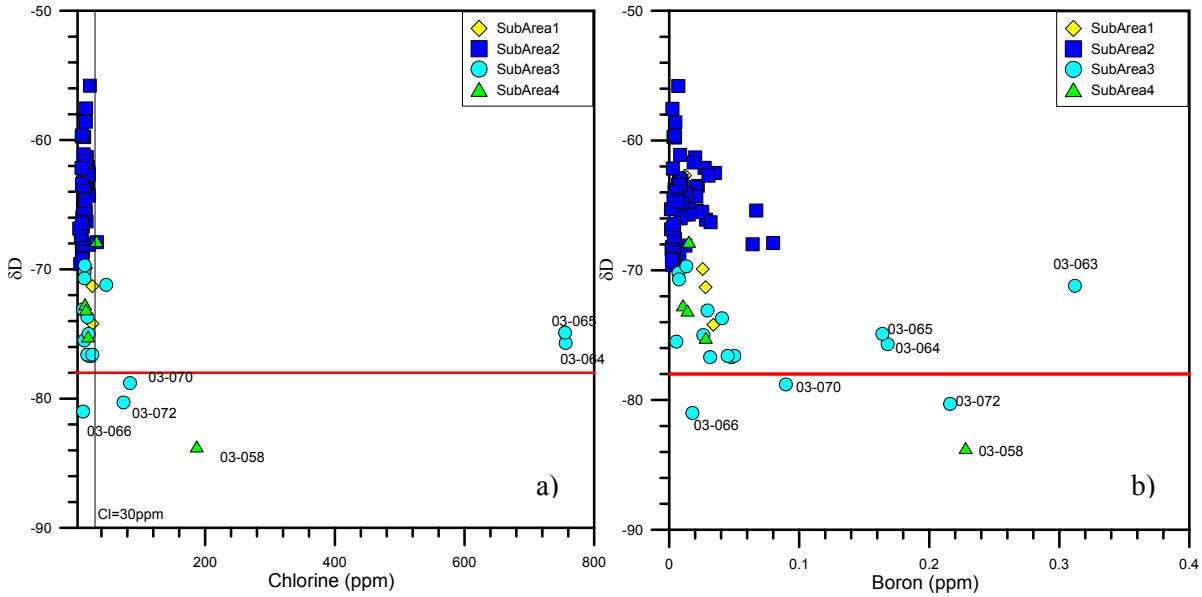

FIGURE 11: The Western Fjords, chlorine and boron concentration versus δD; the solid red line marks the most D depleted mean annual precipitation according to Árnason (1976)

observed correlation is that the older water is from the high mountains, where the soil and the peat is relatively rare, so the main sources of carbon supply in the older waters are atmospheric CO_2 and CO_2 leached from the rock. This is even clearer in Figure 12c, where the relationship between boron and modern ^{14}C concentration is shown, as boron in the water samples originates mostly from the bedrock through which the water has seeped. In Figure 12c, however, two trends (two dash lines) are observed. The first one is through the points of the thermal waters from subareas 2 and 3. The other is through those from subareas 1 and 4. It is suggested that the thermal waters following similar trends also originate from similar groundwater systems, with a similar length of discharge, a similar kind of water-rock interaction and similar chemistry (especially B concentration) of the bedrock in the recharge areas.

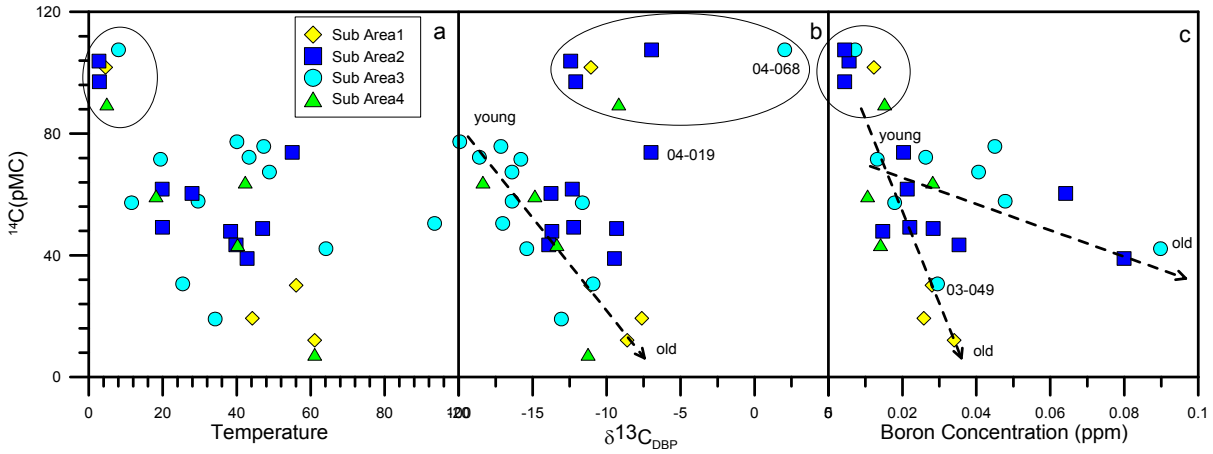

FIGURE 12: Temperature (°C), $\delta^{13}C$ (‰) and boron concentration (ppm) vs. ^{14}C (pMC)

5.1.4 Helium isotope

A helium isotope study was carried out by Hilton et al. (1998) in the Western Fjords. Thirteen out of a total of 16 samples lie in the range of 2Ra to 24Ra and the seven samples that were analyzed for carbon stable isotopes ($\delta^{13}C$) lie in the range of -6 to -16‰. Table 2 shows the samples where carbon isotopes are available and their He isotope results, where R denotes the $^3He/^4He$ ratio of the sample and Ra denotes air $^3He/^4He$, respectively. Hilton et al. (1998) used the correct helium ratio Rc/Ra,

$CO_2/^3He$, carbon isotope and their relationships to reveal the source of the volatiles. They concluded that the source of the mantle-derived volatiles is the degassing of the mantle and that little re-distribution of volatiles from the Icelandic neovolcanic zones takes place via the regional groundwater system. They also proposed that the mechanism by which mantle volatiles are transferred into the Western Fjords thermal water is incipient mantle melting rather than rock leaching, and the mantle input is diluted by the addition of radiogenic helium and isotopically light organic carbon from the uppermost crust. They estimated that approximately 0.04‰ of the total flux of off-axis mantle volatiles are degassed in the region (Hilton et al., 1998).

TABLE 2: Helium and carbon isotope data from the Western Fjords (from Hilton et al., 1998)

Locality	Temperature (°C)	R/Ra	$^{13}C_{(CO2)}$‰ (PBD)
Djúpidalur	67	23.6	-6.8
Flókalundur	37	6.23	-12
Gjögur	63	15.8	-6.53
Hveravík	79	22.3	-13.7
Kirkjuból	61	8.85	-8.01
Laugaland	49	3.4	-16.3
Reykhólar	100	15.2	-8.1

5.2 Hengjing geothermal area in China

5.2.1 Chemical composition of waters

In the Hengjing geothermal area, fourteen samples, including four cold springs with water temperature varying from 18 to 22°C, and ten hot springs 25-73°C, were collected in 1997. The chemical compositions and isotopic data together with measured temperatures are given in Table 2 in Appendix I. Sampling locations are shown in Figure 2. An initial classification of the waters was carried out on the basis of relative contents of the three major anions, Cl, SO_4 and HCO_3 (Figure 13a). None of the waters plot in the fields marked "mature water" or "volcanic water" in the diagram. All the thermal waters plot close to the HCO_3 corner and contain HCO_3 as the predominated anion. This suggests that the thermal waters are of meteoric origin and that absorption of CO_2 diffusing from a deeper level into peripheral groundwater has occurred. The proportion of HCO_3 in the thermal waters is the same as of cold springs, but the thermal waters contain higher SO_4/Cl ratios, probably due to water-rock interaction that increases the SO_4 concentration in the thermal fluids. The data are also plotted in the

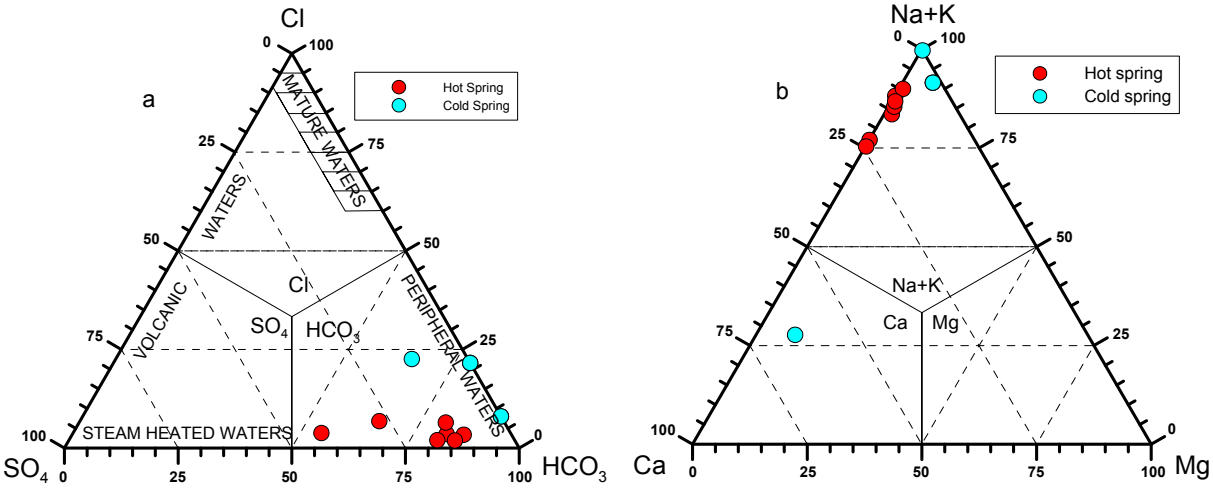

FIGURE 13: Classification of waters from the Hengjing geothermal area on the basis of, a) Relative Cl, SO_4 and HCO_3 content; b) Relative Ca, Mg and Na+K content (in mg/l)

Ca-Mg-(Na+K) triangular diagram (Figure 13b) as relative concentrations. The diagram shows that the geothermal water can be classified as sodium-bicarbonate type. The cold water is classified into sodium-bicarbonate type (Nos. 7 and 8) and calcium-bicarbonate type (No. 10). Clearly, the thermal waters have significantly different chemical properties from the cold waters due to water-rock interaction. However, it is suggested that all waters in this area are of meteoric origin (Sun and Zhang, 2005).

The most convenient method for the simultaneous evaluation of the water-rock equilibration temperatures and the "maturity" of thermal waters is based on the triangular diagram involving the relative Na, K and Mg contents (Giggenbach, 1988). All water samples were plotted in the triangular diagram as shown in Figure 14. In this diagram, the area of partial equilibrium suggests either a mineral that has dissolved but has not attained equilibrium, or a water mixture that has reached equilibrium with dilute unequilibrated water. Points close to the √Mg corner, usually suggest a high proportion of relatively cold groundwater, not "immature". The positions of all the data are classified into two groups: the hot spring group and the cold spring group including samples HJ07, HJ08 and HJ10. Most hot springs of the first group are located in the partially equilibrated and mixed water area or close to it, while the cold waters are located in the immature waters zone. None of the data points suggests full equilibrium. This indicates that the Hengjing waters are not fully mature and the geo-indicators can, therefore, only be used within certain limits. Here, more detailed information is needed on possible processes that have affected the waters. This can be obtained by using the square diagram based on the relative Na, K, Mg and Ca content (Giggenbach, 1988), as shown in Figure 15. It shows that all the water points can be classified into three groups, firstly the mature group close to the full equilibrium line including HJ05, HJ012 and Hj06, secondly the less mature water group located in the centre of the diagram including HJ11, HJ09 and HJ02, and thirdly the cold water group located in the Mg and K corner, including HJ07 HJ08 and HJ10. Using different symbols to represent different water temperature, Figure 15 demonstrates that with increasing temperature the maturity of the waters increases. Isotope

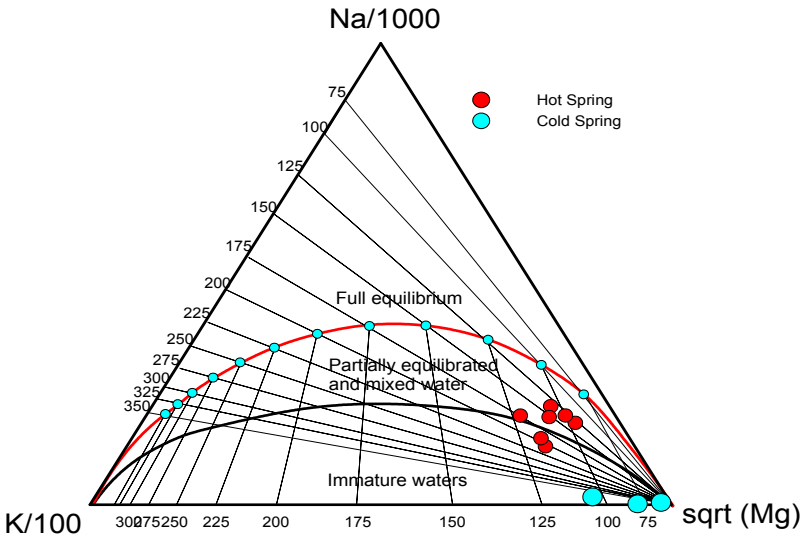

FIGURE 14: Na-K-Mg equilibrium diagram (Arnórsson, 2000) used on the fluids from the Hengjing geothermal area

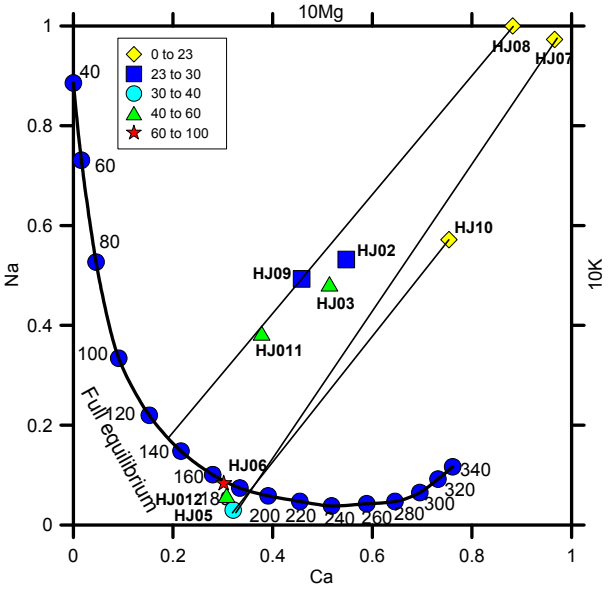

FIGURE 15: Evaluation of Na-K-Mg-Ca equilibration temperatures using $10c_K/(10c_K+c_{Na})$ versus $10c_{Mg}/(10c_{Mg}+c_{Ca})$ (c_i in mg/kg); waters with temperature in the range 0-23°C are represented by diamonds, 23-30°C by squares, 30-40°C by open circles, 40-60°C by triangles and above 60°C by stars

study has shown that the hot water in the Hengjing area is of meteoric origin and a mixture of hot and cold water. The mixing of the thermal waters with surface waters has also been proposed by Sun and Zhang (2005). Figure 15 shows the mixing lines through the hot waters emanating from the cold waters and, with extrapolation, intersecting the full equilibrium line. The temperatures that can be read off, as indicated by these intersection points, suggest that deep water-rock equilibration temperatures are ranging from 130 to 180°C, giving an average value of 155°C.

5.2.2 Stable isotopes of oxygen and hydrogen

In the Hengjing area, the isotopic composition of the cold waters lies in the range of -39 to -55‰ and -5.6 to -7.4‰ for δD and $\delta^{18}O$, respectively. The δD-$\delta^{18}O$ relationship of the cold water is shown in Figure 16, defining the "Local meteoric water line" as δD = 8.33 $\delta^{18}O$ + 8.52, with a correlation coefficient of 0.97. Compared to the global meteoric water line defined by Craig (1961), the local meteoric line has similar slope but the intercept is about 1.5 lower. The δD values of the geothermal waters in this area range from -47 to -57‰, i.e. are more negative than those of the cold springs. The $\delta^{18}O$ values of the thermal waters (-5.9 to -7.2‰) are, however, similar to those of the cold waters. This has been considered to indicate that the origin of the geothermal water is local precipitation from higher latitudes than that of the cold water. The slight oxygen shift, in the range of 0.2-1.0‰, has been explained by interaction between groundwater and the bedrock. However, the oxygen shift is not obvious, especially when the accuracy of the measurements (0.2‰ for oxygen and 3‰ for hydrogen) is taken into consideration. Lack of oxygen shift is taken to indicate low reservoir temperatures, in agreement with Sun and Li (2001) who concluded that the Hengjing area is of a deep circulation type and a low-enthalpy geothermal resource.

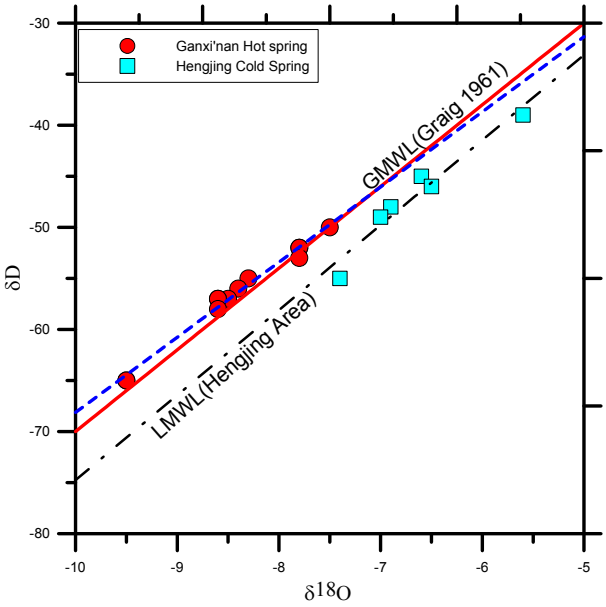

FIGURE 16: The $\delta^{18}O$ vs. δD relationship for cold and hot spring waters in the Hengjing and Gangxi'nan geothermal areas; the best fit for the Gangxi'an data is shown by the dash line and defined as δD = 7.36 $\delta^{18}O$ + 5.49; the cold spring data (squares) from the Hengjing area are shown for comparison, together with the "Global meteoric water line" (Craig, 1961) with solid-line

As mentioned in Section 3, the isotopes of deuterium and oxygen are very useful in studying the origin of geothermal fluids and the recharge areas. They have been widely applied to geothermal studies in China. In the central part of the Jiangxi province, the correlation lines between altitude, *H* (in m), and isotopic composition of local precipitation were defined as (Sun and Li, 2001):

$$\delta D = -25.11 - 0.047H \quad (9)$$

$$\delta^{18}O = -4.82 - 0.0032H \quad (10)$$

where the δD and $\delta^{18}O$ values are expressed in per-mill versus SMOW. According to the isotopic contents of these thermal waters, the recharge altitudes of the thermal waters are in the range of 350-700m (Sun and Li, 2001).

5.2.3 Helium and carbon isotopes

As discussed in Section 3.1.3, helium isotopes are useful for studying the origin of geothermal gases. Helium isotope results were obtained for 4 samples in the area, with the content ranging from 1.90×10^{-6} to 2.95×10^{-6} as shown in Table 2 in Appendix I. These R/Ra ratios, in the range of 1.36 and 2.11, are about a quarter of the MORB (mid-ocean ridge basalt) average level value. Since the $^{3}He/^{4}He$ values for the hot springs are higher than 1 (1Ra), mantle degassing must be occurring, as shown in Figure 17. Thus, the helium isotopes suggest that the Hengjing area is located in a region of degassing of mantle-derived volatiles (Zhou and Zhang, 2001).

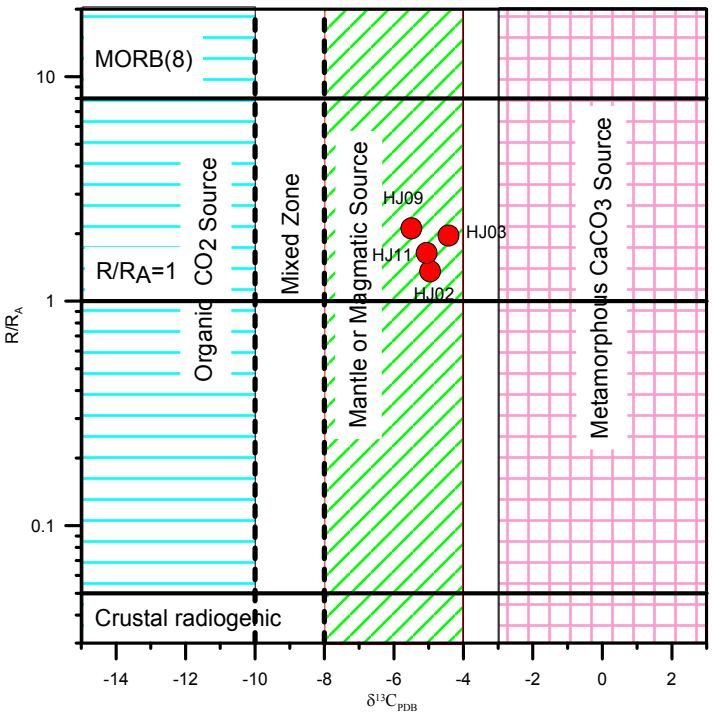

FIGURE 17: The relationship between ^{13}C and the helium ratio for the Hengjing area

Stable carbon isotopes ($\delta^{13}C$) are also very useful in indicating the source of the gases (mantle, crust, subducted sediments or atmosphere). Only four carbon isotope samples were analyzed, as shown in Appendix I. The $\delta^{13}C_{DBP}$ values lie in the range of -6 to -4‰, i.e. somewhat heavier than air (-7‰). In China, the $\delta^{13}C$ (CO_2) values associated with inorganic carbon are normally greater (heavier) than -8‰ and mainly fall in the range of -8 to +3‰, whereas values associated with organic carbon are normally in the range of -8 to ~ -26‰. Values between -10 and -8‰ are considered to be associated with a mixture of inorganic and organic carbon. The $\delta^{13}C$ (CO_2) values associated with magmatic mantle origin carbon normally lie between -8 and -4‰ and the values associated with $CaCO_3$ metamorphous carbon range from -3 to +3‰ (Dai and Dai, 1994). In Figure 17, these typical values for different geological settings are shown together with the data from the Hengjing area group. All the data group together in the mantle or magmatic source zone, where $-8 < \delta\ ^{13}C_{DBP}‰ < -4‰$ and 1 < R/Ra < MORB (8). This is in agreement with the geological observation that carbonate rocks are not found in the area. Thus it is suggested that the gas from the hot springs is of inorganic origin and possible partly of mantle origin.

5.3 The Gangxi'nan geothermal area

5.3.1 Chemical composition of the waters

All of the chemical compositions of water discharged from hot springs in the Gangxi'nan hot spring area, together with measured discharge temperature and isotopes, are given in Table 3 in Appendix I. An initial classification of the waters on the basis of relative contents of Cl-SO_4-HCO_3 and Ca-Mg-(Na+K) is shown in Figure 18. All the samples are located in the HCO_3 corner in Figure 18a and in the Na+K corner in Figure 18b. This indicates that the thermal waters can be classified as Na-HCO_3 water and that all of the waters are highly immature.

The data from the hot springs are shown on the Na-K-Mg ternary diagram in Figure 19. All the hot spring waters plot in the √Mg corner, suggesting that these waters have not attained equilibrium and are immature water, indicating that they have possibly mixed with cold water during upflow. For such waters, the application of solute geothermometers to estimate discharge temperature is not reliable.

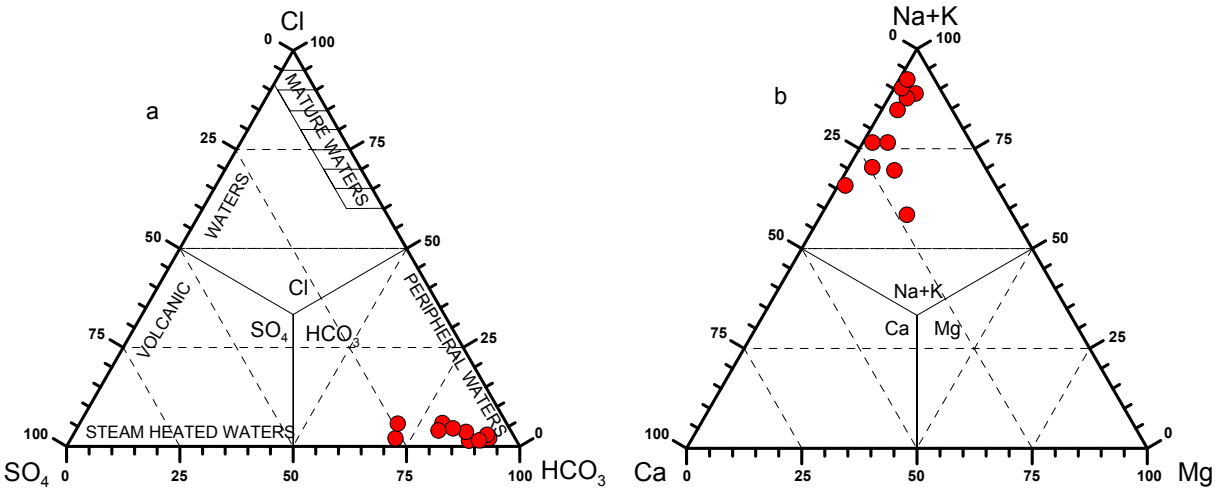

FIGURE 18: Classification of waters from the Gangxi'nan geothermal area on the basis of, a) Relative Cl, SO_4 and HCO_3 content; and b) relative Ca, Mg and Na+K content (in mg/l)

5.3.2 Stable isotopes of oxygen and hydrogen

Figure 16 shows the $\delta^{18}O$ and δD values of thermal waters in the Gangxi'nan area. The figure demonstrates a considerable range both in $\delta^{18}O$ (-9.5 to -7.5‰) and in δD (-65 to -50‰). For comparison the "Global meteoric water line" (GMWL) and the "Local meteoric water line" for the neighbouring Hengjing area are also shown. The best fit through the thermal water data points is $\delta D = 7.36\ \delta^{18}O + 5.49$, very similar to the GMWL. This indicates that the thermal water is of meteoric origin and that temperatures of the geothermal reservoir are low. Using Equations 9 and 10, the altitudes of the recharge areas are estimated to be in the range of 530-1460 m.

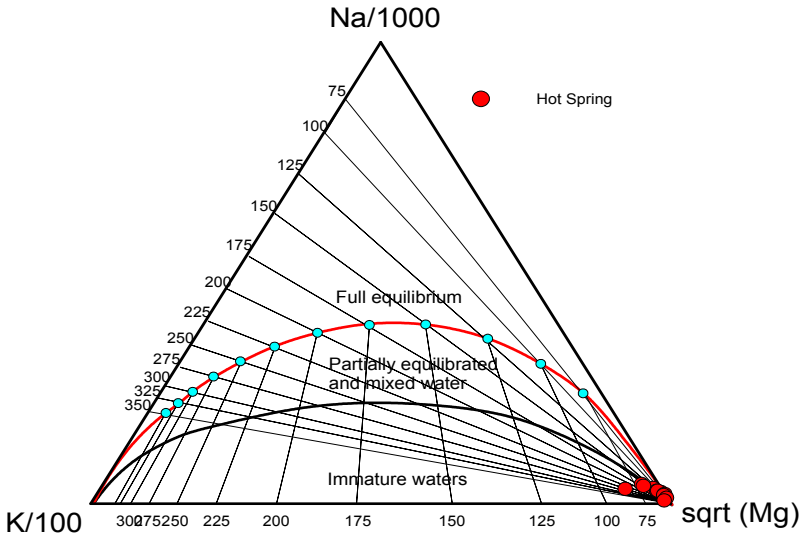

FIGURE 19: Na-K-Mg-Ca equilibrium diagram for waters from the Gangxi'nan geothermal area

5.3.3 Helium and carbon isotopes

Nine samples from five hot springs were analyzed for helium (^3He and ^4He) and carbon isotopes ($\delta^{13}C$) (Table 3). The $\delta^{13}C$ values from the hot springs are in the range of -12.6 to -23.7‰, i.e. considerably lower (more negative) than the atmosphere (-7‰). The $\delta^{13}C$ values associated with organic carbon have been found to be in the range of -8 to -39‰ and most values lie in the range of -12 to -17‰, whereas inorganic carbon falls in the range of -8 to +7‰. Accordingly, CO_2 from the hot springs originates most likely from organic (sedimentary) carbon or from some mixture of organic carbon with either atmospheric carbon or with inorganic carbon. The measured $^3He/^4He$ ratios (R) from the sample range from 1.90×10^{-6} to 2.95×10^{-6} and R/Ra ratios range from 0.05 to 0.13. All of the R/Ra values are smaller than 1, and most of them are less than 0.1. This indicates that the helium in the thermal springs originates from crustal radiogenic production. All the data were plotted in a diagram showing the relationship between helium isotope ratio (R/Ra) and $\delta\ ^{13}C_{DBP}$‰ (Figure 20). It

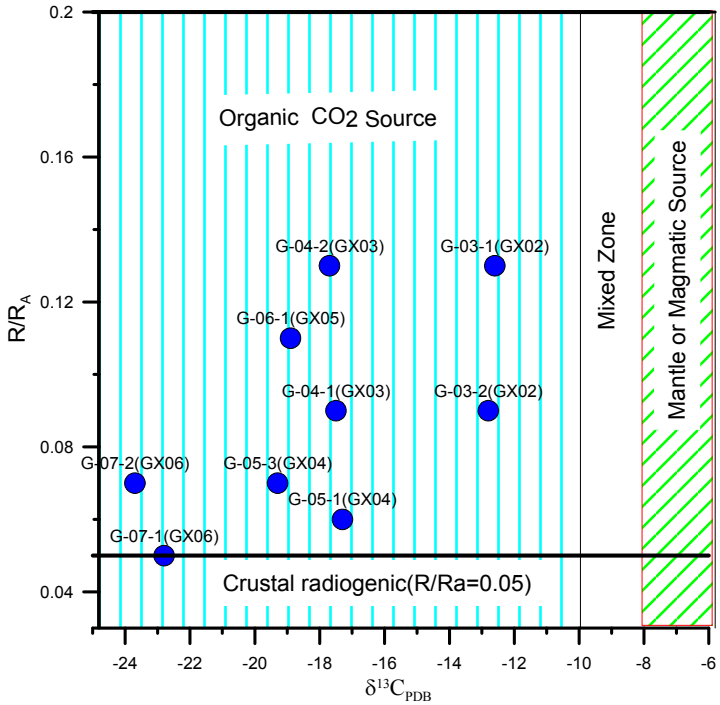

FIGURE 20: The relationship between $\delta^{13}C$ and helium isotope ratio for the Gangxi'nan area

can clearly be seen that all data points fall into the organic CO_2 zone and lie between a typical radiogenic helium value (R/Ra =0.05) and atmospheric helium value (R/Ra=1). Furthermore, there is a tendency for the lighter carbon isotope values to be associated with lower R/Ra ratios, indicating a possible common provenance of radiogenic helium and light carbon. Therefore, the thermal gases can be considered to be of "crustal" radiogenic origin, possibly mixed with the atmosphere.

TABLE 3: Helium and carbon isotopes of hot springs in the Gangxi'nan hot spring area

Sample no.	Spring no.	$\delta 13C_{PDB}$‰	$R=^3He/^4He$	R/Ra
G1	GX02	-12.6	(1.76±0.10)×10-7	0.13
G2	GX02	-12.8	(1.24±0.04)×10-7	0.09
G3	GX03	-17.5	(1.31±0.04)×10-7	0.09
G4	GX03	-17.7	(1.77±0.06)×10-7	0.13
G5	GX05	-17.3	(7.90±0.30)×10-8	0.06
G6	GX05	-19.3	(9.31±0.33)×10-8	0.07
G7	GX09	-18.9	(1.53±0.06)×10-7	0.11
G8	GX10	-22.8	(7.40±0.26)×10-8	0.05
G9	GX10	-23.7	(9.30±0.36)×10-8	0.07

6. DISCUSSION

All data considered for this study are plotted in the Cl-SO4-HCO3 diagram shown in Figure 21. Only few of the waters from Western fjords fall within the mature water zone and three within the zone of volcanic water. Cl and HCO_3 are the dominant anions for all the waters. Cl and HCO_3 are the dominant anions in the thermal waters from the Western Fjords. The source of chloride in these waters is considered for the most part the ocean, seawater spray and aerosols brought down with the precipitation (Arnórsson and Andrésdóttir, 1995). However, the thermal waters from the two areas in China contain only HCO_3 as a dominant anion. The main reasons for this difference are firstly that the Western Fjords are located close to the sea, whereas the areas in China are several hundred kilometres away from the ocean. Secondly, the geology of the areas is very different. Most of the rocks in the Western Fjords are basalt, but in China the rock matrix is more complex, thus, water rock interaction will lead to different water types during the thermal water upflow and mixing with cold water.

The Na-K-Mg ternary diagram provides information about the geothermal water affected by mixing with cold groundwater. Figure 22 shows that all the waters from the Hengjing and Gangxi'nan areas are partially equilibrated or mixed waters and some of the cold water is immature. Also many of the waters from the Western Fjords are partially equilibrated and mixed waters, while some are fully equilibrated. The unequilibrated waters are generally interpreted to have been affected by mixing with cold water. This is in agreement with the oxygen and hydrogen isotope study. The fully equilibrated waters in the diagram suggest that the estimated temperature of the geothermal reservoirs from the Western Fjords is below 100°C. The temperatures of the geothermal reservoir in the Hengjing area, obtained by Ca-Na-K-Mg diagram, range from 130 to 180°C. More information could be achieved by other methods such as with the quartz geothermometer and a silica-enthalpy diagram (Sun and Zhang, 2005). The temperature of the geothermal reservoir in the Gangxi'nan area, however, cannot be obtained by cation geothermometers because all the waters are immature.

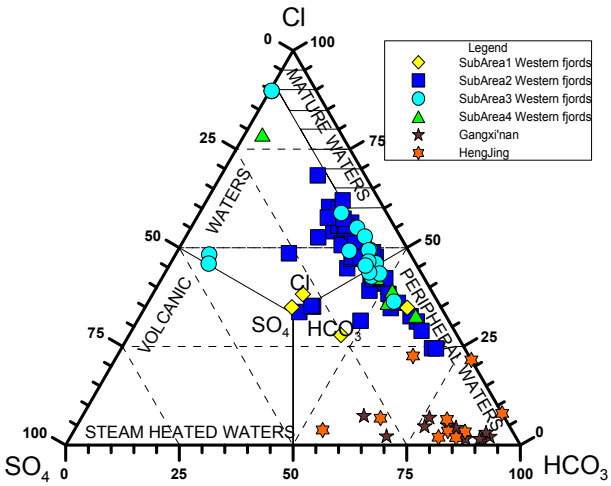

FIGURE 21: Cl-SO4- HCO_3 diagram for waters from all the areas studies

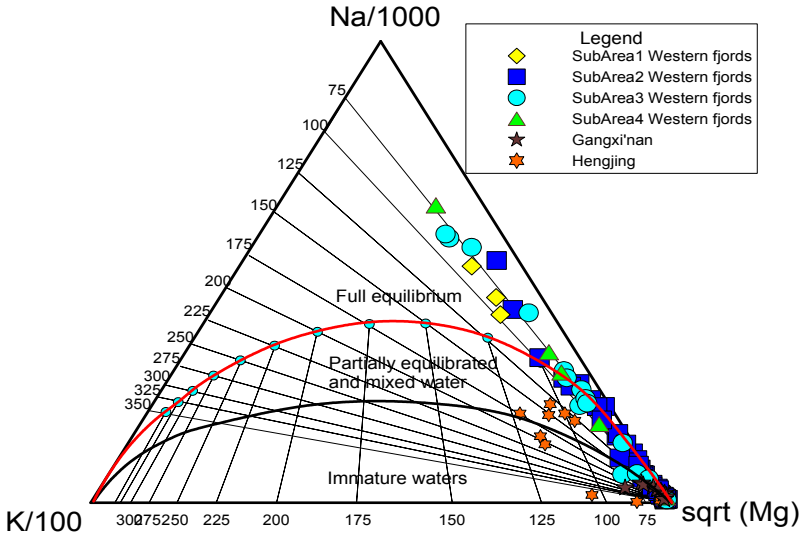

FIGURE 22: Na-K-Mg diagram of samples available from all the three studied areas

All data from the three geothermal areas discussed in this report, are plotted in the δD and $\delta^{18}O$ diagram shown in Figure 23. The δD of the thermal waters from all three places is in the range of -85 to -39‰ and $\delta^{18}O$ ranges from -12 to -5.8‰. The water samples follow the "Global meteoric water line" (GMWL). A linear fit through all the data points from these areas is given as $\delta D = 6.22\ \delta^{18}O - 6.23$. This regression line is very similar with the "Local meteoric water line" ($\delta D = 6.55\ \delta^{18}O - 3.5$) which was defined by Sveinbjörnsdóttir et al. (1995) for $\delta D \geq -10.5$‰ in Iceland. This demonstrates that the thermal waters are of meteoric origin and also indicates that the reservoir temperatures in these areas is relatively low, as no oxygen shift is observed apart from the warm waters in the Hengjing area, which is explained by high CO_2 concentration of the bedrock. This is also in good agreement with other geochemical data that have characterized these areas as low-temperature reservoirs. However, there are some differences between the areas. Firstly, the data points from Iceland are isotopically lighter than those from China. This is due to different latitude and climate regimes. The Western Fjords are located in the high north latitude (about 65-66°), while the Hengjing and Gangxi'nan areas are located at a moderate north latitude (24-26°). The differences in altitude could also be significant. Secondly, as pointed out above, the thermal waters from the Hengjing area may show slight oxygen shift. One possible reason is the high concentration of CO_2 (96.7-99.8%), which can provide more protons for water-rock interaction to cause oxygen isotopic exchange. Even in the same geographical area, the isotope concentration can vary considerably. For

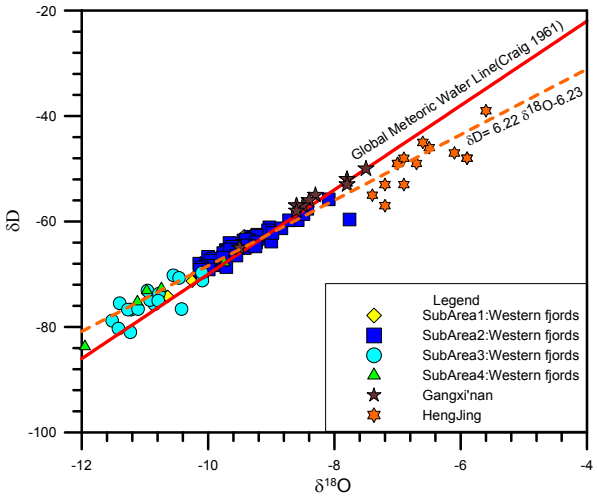

FIGURE 23: The relationship between δD and δ18O for all samples available from the three studied areas; the dash line represents a regression line (δD= 6.22 $\delta^{18}O$ - 6.23) through all the data

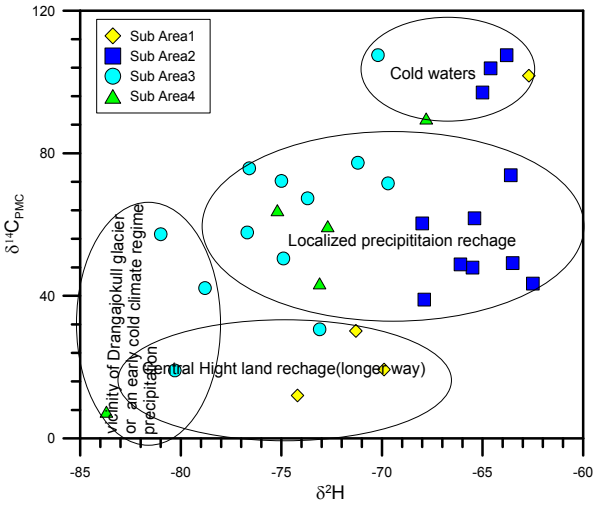

FIGURE 24: δD vs. ^{14}CpMC for the Western Fjords; the data is classified into different groups representing origin and age

example, the thermal waters from different sub areas in the Western Fjords have different δD and $\delta^{18}O$ values. This is taken to suggest that these hot springs have different recharge regimes.

Figure 24 shows δD vs. ^{14}C pMC for the Western Fjords. The waters from the four sub areas in the Western Fjords have different ranges in δD values. According to the regional pattern established by Árnason (1976) for the local precipitation in the Western Fjords and the isotopic signal of the thermal waters, the recharge areas of the thermal waters in subareas 1 and 4 are suggested to be the inner and higher parts of the peninsula, whereas the recharge areas of the thermal waters in subarea 2 and most of the thermal waters in subarea 3 have more local origin, except those with the most negative deuterium values near the eastern coast in subarea 3. The ^{14}C apparent ages of the water samples are in the range of -584 to 20,830 BP, but the percent of modern ^{14}C varies from 7.24 to -107.53. A clear relationship is detected between δD and the ^{14}C apparent age of the groundwater where the isotopic values of the waters increase with increasing ^{14}C pMC (Figure 24). All the data can be classified into four groups according to their relative δD and $\delta^{14}C$ values. The first group is the cold water group, with low temperature and apparently originating from local precipitation. According to the deuterium precipitation contour map (Figure 10), these waters have a "short way" recharge and thus have the highest modern ^{14}C values to indicate their young age. Similarly, the second group, consisting of most waters from subareas 2, 3 and 4, has ^{14}C concentration in the range of 40-80 pMC indicating a relatively young age. It is suggested that their flow channel is short and that they are located close to their discharge. This is in good agreement with the deuterium study, in which the recharge of thermal waters is believed to originate from local precipitation. The third group have more negative δD values and the water is identified with high altitude recharge areas some distance away from the warm springs or it could have some components of water from a colder climate regime when precipitation was more depleted than today. The last group includes waters mostly from the south coast area with the lowest percentage of modern carbon values, indicating that these thermal waters have the longest recharge channel and their recharge regimes are possibly located in the central part of the Western Fjords.

All He isotope data considered in this study and the $\delta^{13}C$ values of gas samples are compiled in Figure 25. The Western Fjords are located ~250 km away from the Icelandic rift-axis. The helium isotope (R/Ra) values in the peninsula are in the range of 3-28 (Hilton et al., 1998). Hilton et al. argued that a mantle-derived input dominates the helium systematic of the nine thermal localities having $^{3}He/^{4}He$ ratios (R/Ra) between those typical of MORB (8±1) and 30, with the highest value matching the most extreme magmatic ratio in this region. They also illustrated the release of radiogenic helium from the

uppermost crust accompanied by additional isotopically light carbon ($\delta^{13}C$ < -6‰) (Figure 25). The total flux of off-axis mantle volatiles degassed is extremely small and is estimated to be approximate 0.04% of the an-axis mantle flux (Hilton et al., 1998). The Hengjing geothermal area is located 800-1000 km away from the convergent boundary between the Philippine plate and the Eurasian plate. The helium isotope values (R/Ra) in the region range between 1 and 2, whereas the $\delta^{13}C$ values fall into the MORB $\delta^{13}C$ range (-5‰ ± 1) (Figure 25). It has been suggested that partial mantle-derived input dominates the helium systematic (Zhou and Zhang, 2001). Gangxi'nan geothermal area is still further away from the convergent boundary, or 1000-1200 km. The isotope (R/Ra) values are in the range of 0.01-0.2, which are much lower than in the other two areas, and most of them fall into the typical radiogenic production value (0.01~0.1). The $\delta^{13}C$ values are very light and lie in the range of -24 to -12‰.

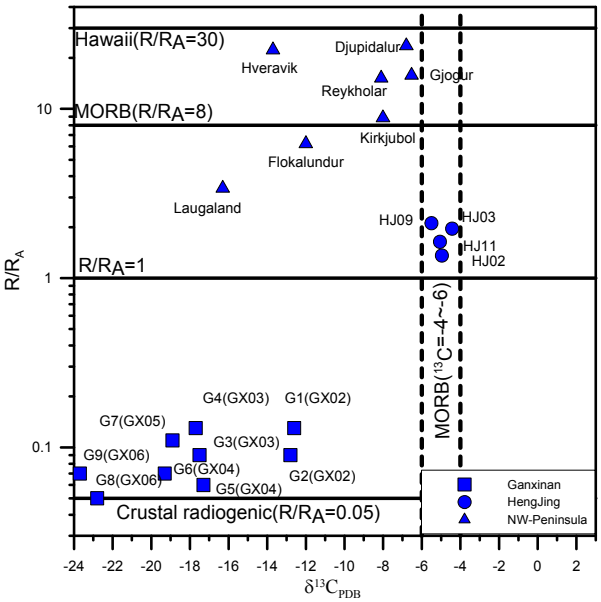

FIGURE 25: Plot of carbon isotope ^{13}C concentration vs. helium ratio (R/Ra) for all the available data from the three study areas

7. CONCLUSIONS

The main conclusions and recommendations can be summarized as follows:

1. The waters from the Western Fjords can be classified as HCO_3 dominated anion type and chlorine type waters. Some of them are mature, but a few fall within the volcanic water zone. Boron, chloride and the B/Cl ratio suggest that the origin of these elements in the hot springs is, apart from the initial concentration of the precipitation, either leaching from the rock with which the water has reacted or mixing with seawater. The thermal waters from Hengjing and Gangxi'nan areas are HCO_3 dominated.

2. According to the Na-K-Mg ternary diagram, some geothermal waters from the Western Fjords seem to have reached equilibrium while others seem to be unequilibrated. The estimated temperature is less than 100°C in this region. The thermal waters from Hengjing area are partially equilibrated or mixed waters. The Na-K-Mg-Ca ternary diagram indicates that the temperatures of the deep thermal water reservoir in the Hengjing area range from 130 to 180°C, while the thermal waters from Gangxi'nan are immature and cannot be used for reservoir temperature estimates.

3. The thermal waters are considered to be of meteoric origin according to the $\delta^{18}O$ and δD relationship. The data from the Western Fjords fit best the predefined Icelandic meteoric water line for waters with $\delta^{18}O$ > -10.5‰, and only a few of the ^{18}O depleted samples plot closer to the predefined meteoric water line for light precipitation.

4. Some of the thermal waters from subareas 1, 3 and 4 in the Western Fjords are more negative in δD than the present local precipitation. It is suggested that their recharge areas lie further away and at a higher altitude. The thermal waters in subarea 2 have a more localized origin.

5. The most depleted deuterium values of thermal waters in the Western Fjords are more depleted than any precipitation on the peninsula today. Two explanations are offered, that the deuterium distribution map by Árnason (1976) of the mean annual precipitation may not be accurate enough, or that the thermal waters may contain a pre-Holocene component.

6. In the Hengjing and Gangxi'nan area, the thermal waters are considered to be of local precipitation origins. The recharge altitudes are around 350-800 m for the hot springs in Hengjing and 530-1460 m for those from Gangxi'nan area.

7. The percentage of modern ^{14}C concentration in geothermal waters in the Western Fjords shows good relationships with temperature, and $\delta^{13}C$ and B concentrations. The relationship between the percentage of modern ^{14}C and δD is used to map the groundwater flow.

8. Helium isotopes $^{3}He/^{4}He$ and $\delta^{13}C$ concentration of gas escaping from the hydrothermal waters show different origins for the three areas studied. Dilution of a mantle helium input occurs in the Western Fjords with additional radiogenic helium and isotopically-light carbon from the uppermost crust. In the Hengjing area, helium and light carbon isotopes show that they could partly be derived from the mantle. Helium in the Gangxi'nan is derived from radiogenic production of the uppermost crust with the addition of very ^{13}C depleted carbon.

ACKNOWLEDGMENTS

I am deeply grateful to the United Nations University and the Government of Iceland for having awarded me the opportunity of attending the Geothermal Training Programme. I would like to especially express my gratitude to Dr. Ingvar B. Fridleifsson, Director of UNU-GTP, for selecting me for this very special programme. My deepest thanks go also to Mr. Lúdvík S. Georgsson, Deputy Director of the UNU-GTP, for his helpful guidance, and Ms. Dorthe, Ms. Thórhildur and Mr. Markús for their efficient help and kindness throughout the training.

My special regards go also to my supervisor, Dr. Árný Erla Sveinbjörnsdóttir. It has been a great honour to be under her guidance and to share her experience and knowledge during the realization of the project. I also owe special thanks to Dr. Kristmannsdóttir and Dr. Arnórsson for they provided the data in my report. I am grateful to Dr. Halldór Ármannsson for his kind and critical comments and to Mrs. Gudrún S. Jónsdóttir for her help in ArcGIS applications. I thank all the lecturers and staff members at Orkustofnun and ISOR – Iceland Geosurvey, for their comprehensive presentations and willingness to share their knowledge and experience.

I owe special thanks to Professors Sun Zhanxue, Wang Guanchai and Liu Jiuhui for their great help and support. I thank the UNU Fellows of 2008 their unforgettable friendship, and thanks also go to my colleagues from the Department of Hydrogeology and Water Recourse, East China Institute of Technology.

Finally, my deepest thanks go to my wife Wang Lei, my daughter Chen Menghan, my family and friends for their moral support during these six months.

REFERENCES

Aravena, R., and Suzuki, O., 1990: Isotopic evolution of river water in the northern Chile region. *Water Resources Research, 26-12,* 2887-2895.

Aravena, R., and Wassennar, L.I., 1993: Dissolved organic carbon and methane in a regional confined aquifer, southern Ontario, Canada: Carbon isotope evidence for associated subsurface sources. *Applied Geochemistry, 8,* 483-493.

Ármannsson, H., and Ólafsson, M., 2000: *Collection of geothermal fluids for chemical analysis*. ÍSOR – Iceland GeoSurvey, Reykjavík, report ISOR-2006/101, 17 pp.

Árnason, B., 1976: *Groundwater systems in Iceland traced by deuterium*. Soc. Sci. Islandica, 42, 236 pp.

Árnason, B., 1977: Hydrothermal systems in Iceland traced by deuterium. *Geothermics, 5*, 125-151.

Arnórsson, S., 1991: Geochemistry and geothermal resources in Iceland, In: D´Amore, F., (coordinator), *Applications of geochemistry in geothermal reservoir development*. UNITAR/UNDP publication, Rome, 145-196.

Arnórsson, S., 1995: Geothermal systems in Iceland: structure and conceptual models – II. Low-temperature areas. *Geothermics, 24,* 603-629.

Arnórsson, S. (ed.), 2000: *Isotopic and chemical techniques in geothermal exploration, development and use. Sampling methods, data handling, interpretation*. International Atomic Energy Agency, Vienna, 351 pp.

Arnórsson, S., and Andrésdóttir, A., 1995: Processes controlling the distribution of boron and chlorine in natural waters in Iceland. *Geochim. Cosmochim. Acta*, *59*, 4125-4146.

Benjaminson, J., 1981: *Chemical composition of geothermal waters in Vestfirdir.* Orkustofnun, Reykjavík, report OS81010/JHD04 (in Icelandic), 121 pp.

Coleman, M.L., Shepard, T.J., Durham, J.J., Rouse, J.E., and Moore, G.R., 1982: Reduction of water with zinc for hydrogen isotope determination. *Anal. Chem., 54,* 993-995.

Craig, H., 1961: Isotope variations in meteoric water. *Science, 153*, 10702-10703.

Craig, H., 1963: The isotopic geochemistry of water and carbon in geothermal areas. In: Tongiorgi, E. (ed.), *Nuclear geology on geothermal areas*. Consiglio Nazionale delle Ricerche, Laboratorio di Geologia Nucleare, Pisa, 17-53.

D'Amore, F., and Arnórsson, S., 2000: Geothermometry. In: Arnórsson, S. (ed.), *Isotopic and chemical techniques in geothermal exploration, development and use. Sampling methods, data handling, interpretation*. International Atomic Energy Agency, Vienna, 152-199.

Dörr, H., Sonntag, S., and Regenberg, W., 1987: Field study on the initial ^{14}C content as a limiting factor in ^{14}C groundwater dating. *Isotope Techniques in Water Resources Development*, IAEA, Vienna, 73-86.

Dai Jinxing and Dai Chensheng, 1994: Geochemical characteristics and carbon and hydrogen isotopic composition. *Science in China, Ser. B, 24-4*, 426-433.

Einarsson, T., 1942: Über das Wesen der heissen Quellen Islands mit einer Übersicht die Tektonik des mittleren Nord-Islands. *Soc. Sci. Islandica, 26*, 91 pp.

Ellis, A.J., and Mahon, W.A.J., 1977: *Chemistry and geothermal systems*. Academic Press, New York, 392 pp.

Epstein, S., and Mayeda, T.K., 1953: Variation of ^{18}O content of waters from natural sources. *Geochim. Cosmochim. Acta, 4*, 213-224.

Fridleifsson, I.B., 1979: Geothermal activity in Iceland. *Jökull 29,* 47-56.

Giggenbach, W.F., 1988: Geothermal solute equilibria, derivation of Na–K–Mg-Ca geoindicators. *Geochim. Cosmochim. Acta, 52*, 2749–2765.

Giggenbach, W.F., 1991: Chemical techniques in geothermal exploration. In: D'Amore, F. (coordinator), *Application of geochemistry in geothermal reservoir development*. UNITAR/UNDP publication, Rome, 119-142.

Hardarson, B.S., Fitton, J.G., Ellam, R.M., Pringle, M.S., 1997: Rift relocation - a geochemical and geochronological investigation of a palaeo-rift in NW Iceland. *Earth Planet. Sci. Lett., 153*, 181-195.

Hilton, D.R., 1996: The helium and carbon isotope systematics of a continental geothermal system: Results from monitoring studies at Long Valley caldera, California, U.S.A. *Chem. Geol., 127*, 269-295.

Hilton, D.R., Grönvold, K., Sveinbjörnsdóttir, Á.E., and Hammerschmidt, K., 1998: Helium isotope evidence for off-axis degassing of the Icelandic hotspot. *Chem. Geol., 149*, 173-187.

Horita, J., 1988: Hydrogen isotope analysis of natural waters using an H_2-water equilibration method: A special indication to brines. *Chem. Geol. (Isotope Geoscience Section), 72,* 89-94.

Jóhannesson, H., and Saemundsson, K., 1999: *Geological map of Iceland in 1:1000000.* Icelandic Institute of Natural History.

Johnsen, S.J., Dansgarrd, W., and White, J., 1989: The origin of arctic precipitation under present and glacial conditions. *Tellus, 41B*, 452-468.

Kristmannsdóttir, H., Arnórsson, S., Sveinbjörnsdóttir Á., and Ármannsson H., 2005: *The project groundwater resources of Iceland. Final report on the results 2005.* University of Akureyri, Deptm. of resources, report HK- 05/04, 25 pp.

Kristmannsdóttir, H., and Sveinbjörnsdóttir, A.E., 1992: Changes of stable isotopes and chemistry of fluids in the low-temperature geothermal field at Bakki-Thóroddstadir, Ölfus, SW-Iceland. *Proceedings of the 7th International Symposium on Water-Rock Interaction, Utah, USA, 2,* 951-954.

Li Xueli, Shi Weijun and Yang Zhongyao, 1992: The formation condition and genesis of the Lushan hotsprings. *J. of East China Geological Institute, 15-3,* 229-233.

Li Xueli and Zhou Wenbin, 1992: Relations between terrestrial heat and uranium deposits in Jiangxi Province, China. *Proceedings of the 7th International Symposium on Water-Rock Interaction, Utah, USA, 2,* 1597-1599.

McDougall, I., Kristjansson, L., Saemundsson, K., 1984: Magnetostratigraphy and geochronology of northwest Iceland. *J. Geophys. Res., 89*, 7029-7060.

McNichol, A.P., Jones, G.A., Hutton, D.L., and Gagnon, A.R., 1994: The rapid preparation of seawater CO_2 for radiocarbon analysis at the national ocean Sciences AMS facility. *Radiocarbon, 36,* 237-246.

Mook, W.G., 1980: Carbon-14 in hydrological studies. In: Fritz, P., and Fontes, J.Ch., (eds), *Handbook of Environmental isotope Geochemistry. The Terrestrial Environment*. Elsevier, Amsterdam, 49-74.

Nicholson, K., 1993: *Geothermal fluids: chemistry and exploration techniques.* Springer-Verlag, Berlin, 268 pp.

Paces, T. (editor), 1991: *Fluid sampling for geothermal prospecting*. UNITAR/UNDP publication, Rome, 94 pp.

Pálmason, G., and Saemundsson, K., 1979: Summary of conductive heat flow in Iceland. In: Cermak, V., and Rybach, L. (eds.), *Terrestrial heat flow in Europe*. Springer-Verlag, Berlin, 218-220.

Pang Z., and Ármannsson, H. (editors), 2006*: Analytical procedures and quality assurance for geothermal water chemistry*. UNU-GTP, Iceland, Report 1, 172 pp.

Sun Zhanxue, 1998: Geothermometry and chemical equilibrium of geothermal fluids from Hveragerdi, SW-Iceland, and selected hot springs Jiangxi province, SE-China. Report 14 in: *Geothermal training in Iceland 1998.* UNU-GTP, Iceland, 373-402.

Sun Zhanxue and Li Xueli, 2001: Studies of geothermal waters in Jiangxi Province using isotope techniques. *Science in China, Ser. E*, *44*, 144-150.

Sun Zhanxue, Li Xueli and Shi Weijun, 1992: Isotope hydrogeochemistry of thermal waters in Jiangxi Province. *J. of East China Geological Institute*, *4*, 20-26.

Sun Zhanxue and Zhang Weimin, 2005: Subsurface temperature estimation of geothermal reservoirs in the Hengjing hot spring area, Jiangxi Province, SE-China. *Proceedings of the World Geothermal Congress 2005, Antalya, Turkey*, CD, 4 pp.

Sveinbjörnsdóttir, Á.E., and Arnórsson, S., 2007: Isotope heterogeneity of Pre-Holocene ground water in Iceland. *Proceedings of the 12th International Symposium on Water-Rock Interaction 2004, Kunming, China,* Taylor & Francis Group, London, 789-792.

Sveinbjörnsdóttir, Á.E., Arnórsson, S., and Heinemeier, J., 2001: Isotopic and chemical characteristics of old "ice age" groundwater in North Iceland. *Proceedings of the 10th International Symposium on Water-Rock Interaction, Villasimius, Italy, A.A. Balkema, Rotteredam,* 205-208.

Sveinbjörnsdóttir, Á.E., Arnórsson, S., Heinemeier, J., and Boaretto, E., 2000: ^{14}C ages of groundwater in Iceland. *Proceedings of the World Geothermal Congress 2000, Kyushu-Tohoku, Japan,* 1797-1802.

Sveinbjörnsdóttir, Á.E., Heinemeier, J., and Arnórsson, S., 2005: Isotopic characteristics ($\delta^{18}O$, δD, $\delta^{13}C$, ^{14}C) of thermal waters in the Mosfellssveit and Reykjavík low-temperature areas, Iceland. *Proceedings of the World Geothermal Congress 2005, Anatalya, Turkey*, CD, 5 pp.

Sveinbjörnsdóttir, Á.E., Heinemeier, J., Arnórsson, S., and Boaretto, E., 1998: Geochemistry of natural waters in Skagafjördur, N-Iceland. II. Isotopes. *Proceedings, of the 9th Symposium on Water-Rock Interaction, Taupo, New Zealand, A.A. Balkema, Rotterdam,* 653-656.

Sveinbjörnsdóttir, Á.E., Heinemeier, J. Rud, N. and Johnsen, S.J., 1992: ^{14}C anomalies observed for plants growing in Icelandic geothermal waters. *Radiocarbon, 34,* 696-703.

Sveinbjörnsdóttir, Á.E., Johnsen, S.J., and Arnórsson, S., 1995: The use of stable isotopes of oxygen and hydrogen in geothermal studies in Iceland. *Proceedings of the World Geothermal Congress 1995, Florence, Italy, 2,* 1043-1048.

Sveinbjörnsdóttir, Á.E., Johnsen, S.J., Kristmannsdóttir H., and Ármannsson, H., 2004: Isotopic characteristic of natural waters in the Southern Lowlands of Iceland. *Proceedings of the 11th International Symposium on Water-Rock Interaction 2004, New York, USA,* Taylor & Francis Group, London, 1404-1405.

Taylor, C.B., 1994: Hydrology of the Poverty Bay flats aquifers, New Zealand: recharge mechanisms, evolution of the isotopic composition of dissolved inorganic carbon, and ground-water ages. *J. of Hydrology, 158*, 151-158.

Tómasson, H., Fridleifsson, I.B., and Stefánsson, V., 1975: A hydrological model for the flow of thermal water in southwestern Iceland with special reference to the Reykir and Reykjavík thermal areas. *2nd United Nations Symposium on the Development and Use of Geothermal Resources, San Francisco, Ca, 2,* 643-648.

Wang Jiyang, and Sun Zhanxue, 2001: Brief review on the development of isotope hydrology in China. *Science in China, Ser. E, 44,* 1-5.

Wang Xianbin, 1989: *Rare gas isotopic geochemistry and cosmochemistry*. Science Press, Beijing, 595 pp.

Zhou Wenbin, and Zhang Weimin, 2001: Gas isotopes and geochemistry of hot springs in Hengjing, Jingxi Province. *Science in China, Ser. E, 44,* 151-159.

APPENDIX I: Analyses of natural waters from the study areas

TABLE 1: Partial analysis of natural waters from the Western Fjords in Iceland, conc. in ppm

Sample no.	Temp.	pH	SiO_2	Na^+	K^+	SO_4^{2-}	TDS	Cl^-	B	Ca^{2+}	Mg^{2+}	CO_2e	δD (‰)	$\delta^{18}O$ (‰)	^{14}CageBp	^{14}CpMC	$^{13}C_{DBP}$ (‰)
7957	100.0		100.5	58.6	2.1	33.0	276.0	32.5	0.0380								
7958	84.0		106.9	55.2	2.1	31.4	251.0	28.8	0.0270								
7959	18.0		36.5	30.0	0.2	6.7	118.0	18.8	0.0450								
7960	84.0		70.9	184.0	4.3	42.1	769.0	390.0	0.1600								
7961	72.0		49.0	716.0	17.3	297.6	4430.0	2460.0	0.3700								
7962	40.0		33.1	26.9	0.3	6.5	102.0	15.9	0.0160								
8524	63.0		73.7	53.9	0.8	34.7	214.0	30.4	0.0980								
8524	76.0		107.9	81.7	0.6	16.2	333.0	93.5	0.2400								
8524	58.0		55.0	39.5	0.8	6.8	142.0	17.6	0.0440								
8524	41.0		38.7	33.0	0.3	5.2	113.0	16.9	0.0630								
8711	38.0	9.77	24.4	23.9	0.3	8.3	88.2	13.4	0.0151	2.3	0.0	15.1	-64.20	-9.53			
8712	22.0	9.9	16.7	18.0	0.2	3.1	71.0	12.8	0.0077	3.3	0.0	16.8	-62.90	-9.33			
8713	20.0	9.65	17.3	18.1	0.2	3.2	74.7	12.6	0.0095	3.2	0.0	20.0	-63.30	-9.20			
8714	39.0	9.94	40.7	32.4	0.4	6.1	122.6	19.0	0.0273	2.4	0.0	21.4	-62.10	-9.04			
8715	43.0	9.93	39.0	28.3	0.3	4.3	111.3	17.4	0.0201	2.5	0.0	19.2	-61.30	-8.84			
8716	27.5	9.24	26.3	21.0	0.2	3.3	92.6	12.7	0.0085	3.0	0.0	25.9	-61.10	-9.03			
8717	34.0	9.84	36.7	27.3	0.3	4.8	120.7	16.3	0.0189	2.2	0.0	32.8	-61.70	-9.05			
8718	44.0	9.76	47.4	27.8	0.5	12.5	117.9	15.6	0.0254	2.1	0.0	11.6	-65.50	-9.58			
8719	51.0	9.84	57.9	34.2	0.6	16.2	141.7	17.2	0.0319	2.3	0.0	12.7	-66.30	-9.59			
8720	24.5	9.75	30.2	19.9	0.5	4.2	84.5	15.2	0.0135	2.1	0.1	12.1	-64.70	-9.38			
8721	19.5	9.55	27.6	16.2	0.6	3.8	71.8	14.3	0.0107	1.9	0.2	7.1	-65.70	-9.66			
8722	14.5	9.59	42.2	23.6	1.0	4.0	98.5	20.2	0.0125	0.7	0.0	6.7	-68.10	-9.84			
8723	6.0	9.19	18.2	9.1	0.5	1.8	48.7	11.3	0.0037	2.4	0.3	5.0	-68.30	-9.92			
8724	5.0	9.17	18.6	9.6	0.5	1.8	50.1	11.1	0.0028	2.1	0.3	6.1	-66.70	-10.00			
8725	14.0	9.04	35.6	20.1	0.5	3.3	82.6	14.1	0.0149	0.7	0.1	8.1	-64.70	-9.59			
8726	14.0	8.87	32.5	17.8	0.6	2.4	73.3	14.1	0.0089	0.7	0.1	5.1	-64.60	-9.47			
8727	14.0	9.12	31.0	19.8	0.4	2.6	74.8	13.7	0.0094	1.0	0.1	6.0	-63.10	-9.28			
8728	11.0	8.9	20.5	16.5	0.6	2.6	62.4	14.2	0.0075	0.6	0.4	6.8	-65.00	-9.42			
8729	11.0	8.93	21.8	13.7	0.3	2.4	65.3	18.4	0.0069	2.0	0.2	6.4	-63.40	-9.32			
8730	6.0	8.59	17.8	10.5	0.4	2.4	53.9	15.6	0.0042	3.1	0.5	3.5	-63.80	-9.00			
8731	19.0	9.02	36.6	24.9	0.4	4.6	98.2	20.8	0.0209	1.7	0.1	8.7	-64.30	-9.27			
8732	24.5	8.94	39.4	23.7	1.0	7.1	102.3	20.5	0.0303	2.0	0.2	8.2	-62.70	-9.23			
8733	6.0	8.57	18.2	17.4	0.4	3.5	68.1	22.1	0.0071	2.0	0.3	4.0	-55.80	-8.09			
8947	25.0		30.3	95.0	0.7	5.9	157.0	12.4	0.0670				-65.40	-9.66			
8948	30.0		32.4	24.9	0.2	5.3	88.0	12.0	0.0130				-64.10	-9.66			

Sample no.	Temp.	pH	SiO_2	Na^+	K^+	SO_4^{2-}	TDS	Cl^-	B	Ca^{2+}	Mg^{2+}	CO_2e	δD (‰)	$\delta^{18}O$ (‰)	^{14}CageBp	^{14}CpMC	$^{13}C_{DBP}$ (‰)
8949	5.0		8.0	9.1	0.3	4.2	45.0	8.5	0.0028				-66.80	-9.75			
8950	3.0		12.1	8.6	0.5	5.4	56.0	11.0	0.0022				-68.20	-9.77			
8951	12.0		25.8	29.5	0.1	6.2	92.0	15.3	0.0150				-65.70	-9.70			
8952	10.0		19.4	15.4	0.4	5.2	66.0	9.6	0.0046				-67.60	-9.94			
8953	7.0		22.6	9.3	0.5	4.3	54.0	7.6	0.0035				-67.00	-9.91			
8954	8.0		20.0	9.6	0.6	4.3	54.0	8.5	0.0038				-67.40	-9.96			
8955	19.0		27.2	16.3	0.6	4.9	72.0	10.4	0.0088				-66.00	-9.76			
8956	14.0		31.9	18.2	0.7	4.2	79.0	11.6	0.0096				-64.80	-9.62			
8957	6.0		10.3	7.6	0.4	3.6	46.0	9.6	0.0018				-68.40	-10.00			
8958	6.0		25.3	10.4	0.6	3.5	57.0	7.1	0.0024				-69.60	-10.10			
8959	9.0		30.4	17.3	0.3	3.7	71.0	9.6	0.0067				-69.50	-10.10			
8960	9.0		31,7	17.6	0.3	5.3	75.0	10.7	0.0079				-68.70	-10.10			
8961	21.0		15.5	17.1	0.2	4.7	63.0	10.3	0.0074				-63.60	-9.35			
8962	21.0		17.2	18.3	0.2	5.2	67.0	10.1	0.0084				-63.40	-9.40			
8963	37.0		33.2	25.3	0.8	6.7	93.0	12.0	0.0140				-65.30	-9.65			
9002	12.5	6.12	2.9	3.6	0.5	1.5	17.6	5.7	0.0015	0.7	0.4	2.4	-66.85	-9.77			
9003	12.5	5.97	6.1	6.9	0.5	2.1	33.5	9.1	0.0029	1.6	0.7	6.4	-62.16	-8.98			
9004	11.5	6.65	5.9	6.7	0.3	2.2	29.9	9.4	0.0033	1.3	0.6	3.4	-59.72	-8.58			
9005	11.8	7.17	10.4	10.6	0.5	3.0	53.9	13.4	0.0046	3.8	1.2	10.9	-59.77	-8.72			
9006	13.0	7.08	7.7	8.5	0.5	2.5	38.7	10.5	0.0043	1.8	0.7	6.5	-59.62	-7.76			
9007	17.8	7.23	13.4	10.3	0.8	3.3	65.3	16.4	0.0026	5.6	1.8	13.7	-57.56	-8.43			
9008	11.6	6.86	9.1	9.8	0.6	2.8	48.4	16.0	0.0048	2.1	1.4	6.5	-58.59	-8.49			
9009	9.6	6.8	7.7	9.3	0.4	2.8	43.8	13.3	0.0049	2.1	1.1	7.1	-63.94	-9.24			
9010	6.2	6.78	13.4	9.1	0.7	2.7	49.3	13.8	0.0034	2.4	1.1	6.0	-64.53	-9.38			
9011	5.2	6.92	13.7	9.4	0.5	2.6	51.1	11.1	0.0036	3.3	0.9	9.5	-68.64	-9.71			
9012	6.0	6.68	11.2	7.6	0.5	2.4	43.9	10.1	0.0023	2.3	1.0	8.8	-69.08	-9.99			
9013	10.0	6.87	10.0	8.2	0.4	2.7	42.2	10.1	0.0038	1.9	1.1	7.7	-66.45	-9.55			
9014	5.0	6.75	9.7	7.4	0.4	2.2	39.8	10.3	0.0021	2.6	0.8	6.3	-69.18	-10.13			
9015	12.2	6.92	10.8	13.9	0.6	3.7	60.9	14.3	0.0071	2.5	1.2	13.9	-64.71	-9.25			
03-047	4.6	6.98	8.8	11.2	<0.50	3.8		17.8	0.0123	7.3	1.5	21.3	-62.70	-9.43	-140	101.8	-11.06
03-048	61.1	9.77	118.8	57.3	1.0	24.5		26.1	0.0340	2.7	<0.002	17.4	-74.20	-10.64	16980	12.1	-8.61
03-049	56.1	9.71	111.2	50.2	1.1	19.5		26.0	0.0280	2.9	0.0	16.2	-71.30	-10.25	9630	30.2	-11.08
03-050	44.2	9.7	88.3	41.8	0.7	14.8		16.2	0.0258	2.7	<0.002	19.5	-69.90	-10.17	13210	19.3	-7.62
03-051	38.3	10.21	25.6	22.8	<0.50	4.3		12.3	0.0147	2.4	<0.002	10.7	-65.50	-9.64	5910	47.9	-13.70
03-052	39.8	10.12	40.7	33.4	<0.50	5.6		20.3	0.0353	2.5	0.0	12.0	-62.50	-9.22	6700	43.4	-13.91
03-053	2.8	7.88	12.0	7.9	<0.50	2.2		13.5	0.0056	2.6	1.3	8.6	-64.60	-9.51	-302	103.8	-12.43
03-054	2.9	7.92	14.5	6.9	0.6	2.0		11.8	0.0044	2.6	0.9	7.9	-65.00	-9.52	239	97.1	-12.09

Sample no.	Temp.	pH	SiO_2	Na^+	K^+	SO_4^{2-}	TDS	Cl^-	B	Ca^{2+}	Mg^{2+}	CO_2e	δD (‰)	$\delta^{18}O$ (‰)	^{14}CageBp	^{14}CpMC	$^{13}C_{DBP}$ (‰)
03-055	47.0	9.71	48.6	29.1	0.5	11.6		14.5	0.0283	2.1	0.0	11.0	-66.10	-9.75	5760	48.8	-9.33
03-056	19.9	9.56	25.3	16.5	0.5	3.8		13.9	0.0213	1.8	0.2	7.0	-65.40	-9.72	3870	61.8	-12.32
03-057	19.9	9.59	32.8	23.1	<0.50	3.9		19.3	0.0220	1.6	0.1	8.6	-63.50	-9.34	5695	49.2	-12.23
03-058	61.1	9.44	85.1	133.6	1.7	41.3		187.0	0.2280	17.5	0.0	6.7	-83.70	-11.95	20830	7.5	-11.25
03-059	4.9	7.68	15.8	20.6	0.5	6.5		32.3	0.0152	16.0	3.0	43.1	-67.80	-9.74	870	89.7	-9.18
03-060	18.2	10.02	17.0	22.4	<0.50	3.6		14.7	0.0106	2.6	0.0	11.8	-72.70	-10.74	5640	59.5	-14.85
03-061	40.2	9.87	40.3	29.8	<0.50	5.0		16.2	0.0141	2.5	0.0	17.1	-73.10	-10.97	6680	43.5	-13.36
03-062	42.3	9.8	45.1	34.8	<0.50	4.3		19.4	0.0282	1.7	0.0	18.7	-75.20	-11.12	3579	64.1	-18.36
03-063	40.1	9.69	41.1	49.5	0.6	8.0		47.3	0.3120	4.3	0.0	18.1	-71.20	-10.09	2065	77.3	-19.93
03-064	87.1	8.82	82.0	300.4	5.0	82.8		756.0	0.1680	186.1	0.0	2.8	-75.70	-10.85			-16.40
03-065	93.5	8.84	80.7	301.4	5.0	82.4		755.0	0.1640	191.6	0.0	2.5	-74.90	-10.92	5490	50.5	-17.03
03-066	11.6	9.31	38.8	14.4	1.2	1.8		11.7	0.0179	0.6	0.0	5.6	-81.00	-11.23	4475	57.3	-11.64
03-067	29.6	9.51	37.3	29.7	1.2	4.6		24.2	0.0478	3.2	0.2	17.1	-76.70	-11.22	4405	57.8	-16.39
03-068	8.0	7.36	7.8	8.3	<0.50	2.4		14.0	0.0072	2.3	1.6	8.6	-70.20	-10.55	-584	107.5	2.04
03-069	3.3	8.68	13.6	7.8	0.7	2.0		13.4	0.0056	2.9	1.0	7.2	-75.50	-11.40			
03-070	64.1	9.57	57.0	93.2	0.9	77.0		84.0	0.0898	10.3	0.0	9.3	-78.80	-11.52	6930	42.2	-15.40
03-071	9.0	7.33	7.9	8.1	<0.50	2.4		13.7	0.0076	2.3	1.6	8.4	-70.70	-10.46			
03-072	34.2	9.56	79.5	101.4	1.2	73.3		74.0	0.2160	2.2	0.0	9.8	-80.30	-11.42	13310	19.1	-13.06
03-073	25.4	9.91	25.0	20.2	<0.50	3.0		11.4	0.0295	0.6	0.0	6.3	-73.10	-10.96	9510	30.6	-10.92
03-074	42.8	9.86	47.5	33.2	0.5	4.5		20.4	0.0315	1.4	0.0	13.7	-76.70	-11.27			
03-075	48.8	9.91	40.0	30.7	<0.50	4.9		18.2	0.0406	2.8	0.0	14.1	-73.70	-10.78	3174	67.4	-16.40
03-076	43.3	9.85	50.8	35.2	0.5	4.3		20.0	0.0263	2.4	0.0	15.7	-75.00	-10.79	2615	72.2	-18.60
03-077	44.3	9.96	52.9	36.2	<0.50	4.7		18.0	0.0501	1.4	0.1	13.3	-76.60	-11.11			
03-078	47.3	9.47	44.1	31.1	0.5	6.5		26.0	0.0450	4.8	0.0	17.8	-76.60	-10.42	2230	75.8	-17.15
03-079	19.4	9.77	19.8	22.2	<0.50	3.7		14.1	0.0132	2.9	0.2	15.1	-69.70	-10.10	2690	71.6	-15.80
04-016	27.9	10.24	44.6	35.4	0.2	4.9		14.0	0.0641	1.6	0.0	8.9	-68.00	-10.14	4060	60.3	-13.76
04-017	42.8	9.99	46.7	52.8	0.4	18.0		32.9	0.0800	2.5	0.0	12.1	-67.90	-10.03	7570	39.0	-9.47
04-018		7.02	8.5	9.3	0.2	2.7		11.7	0.0044	3.7	1.5	16.6	-63.80	-9.39	-582	107.5	-6.96
04-019	55.0	9.81	42.4	27.7	0.3	4.4		15.5	0.0203	1.3	0.1	9.3	-63.60	-9.44	2436	73.8	-7.00

TABLE 2: Chemical data isotopes of springs in Hengjing geothermal area (concentrations in mg/l)

Spring no.	Type	Temp. (°C)	pH/°C	CO_2	SiO_2	Ca^{2+}	Mg^{2+}	K^+	Na^+	Cl^-	SO_4^{2-}	HCO_3^-	TDS	δD (‰)	δ18O (‰)	d = $8_*{}^{18}$O-D	$\delta^{13}C$ PDB (‰)	$^3He/^4He$ (10^{-6})	R/R_a
HJ01	Cold spring													-55	-7.4	-4.2	-	-	-
HJ02	Hot spring	25	6.52/20	1263.0	99.0	138.5	15.7	84.6	698.6	81.2	325.0	1886.1	2286.7	-57	-7.2	-0.6	-4.96	1.90±0.06	1.36
HJ03	Hot spring	48	6.67/20	725.3	94.0	117.1	11.0	71.8	679.1	70.2	764.9	1004.2	2216.1	-53	-6.9	-2.2	-4.43	2.74±0.12	1.96
HJ04	Hot spring	40												-49	-6.7	-4.6	-	-	-
HJ05	Hot spring	37	6.74/20	22.0	78.0	29.1	0.1	4.4	93.6	8.5	26.5	217.0	270.7	-53	-7.2	-4.6	-	-	-
HJ06	Hot spring	73	7.30/20	8.8	81.0	9.9	0.1	3.1	71.5	8.5	17.0	106.1	163.1	-47	-6.1	-1.8	-	-	-
HJ07	Cold spring	18	6.72/20	21.0	19.0	0.1	0.4	3.7	1.3	2.2	0.0	8.0	11.6	-46	-6.5	-6	-	-	-
HJ08	Cold spring	21	6.92/20	16.0	17.0	0.0	0.0	1.5	2.0	2.2	0.0	25.2	18.3	-39	-5.6	-5.8	-	-	-
HJ09	Hot spring	27	6.50/20	547.0	43.0	106.9	10.4	82.0	969.8	50.7	350.0	2253.1	2696.3	-48	-5.9	0.8	-5.50	2.95±0.10	2.11
HJ10	Cold spring	22	6.18/20	16.0	15.0	33.4	4.5	3.4	11.1	22.0	12.0	63.4	118.0	-49	-7	-7	-	-	-
HJ11	Hot spring	48	6.77/20	722.0	135.0	107.8	6.7	43.2	711.2	35.1	300.0	1428.1	1918.1	-48	-5.9	0.8	-5.06	2.30±0.08	1.64
HJ12	Hot spring	44	6.63/20	250.0	82.0	52.3	0.3	6.9	154.4	28.7	115.0	276.8	496.0	-49	-7	-7	-	-	-
HJ13	Cold spring	20												-48	-6.9	-7.2	-	-	-
HJ14	Cold spring	19												-45	-6.6	-7.8	-	-	-

TABLE 3: Chemical composition of springs in Gangxi'nan geothermal area (concentrations in mg/l)

Spring no.	Temp. (°C)	pH	Cond. (μs)	Ca^{2+}	Mg^{2+}	K^+	Na^+	Al	Cl^-	SO_4^{2-}	HCO_3^-	CO_3^{2-}	CO_2	SiO_2	$\delta^{18}O$‰	δD‰
GX02	43.9	6.82	675.0	21.2	1.0	6.9	35.8	0.0	4.8	23.8	280.9	0.0	42.0	89.7	-7.50	-50.0
GX03	37.7	8.91	395.0	2.8	2.5	0.7	41.4	0.0	2.1	15.4	119.0	10.1	0.0	56.6	-8.30	-55.0
GX04	41.0	7.67	455.0	10.4	1.0	1.4	35.8		4.2	11.5	186.1	0.0	84.0	64.7	-7.80	-52.0
GX05	83.8	8.61	713.0	4.0	1.9	1.5	40.4		2.8	36.5	89.4	9.5	0.0	117.2	-8.40	-56.0
GX06	39.0	8.80	315.0	5.2	1.5	1.1	36.0		3.5	9.6	67.1	15.4	0.0	63.9	-8.50	-57.0
GX07	42.5	8.47	286.0	12.0	2.5	0.0	34.4	0.2	4.8	11.5	53.2	11.9	4.2	46.1	-7.80	-52.0
GX08-1	38.0	8.67	178.1	6.4	1.9	0.4	26.7	0.7	3.5	9.6	58.0	5.9	4.2	67.9	-8.60	-57.0
GX08-2	39.0	8.91	945.0	7.6	3.9	0.2	26.1	0.2	2.9	11.5	47.1	10.7	0.0	62.3	-8.60	-57.0
GX09-1	76.0	8.48	655.0	4.0	0.8	2.8	41.2	0.9	4.7	9.2	138.9	7.1	0.0	107.5	-9.50	-65.0
GX09-2	84.0														-9.50	-65.0
GX10	40.0	9.40	418.0	2.4	0.7	2.5	34.8	2.0	6.9	28.8	58.0	26.1	0.0	101.0	-8.60	-58.0
GX11	53.7	7.49	188.0	8.4	6.8	2.1	19.3	0.7	0.7	3.8	41.7	0.0	0.0	62.3	-7.80	-53.0